Biosystems Engineering 270 (2026) 104556

Contents lists available at ScienceDirect

Biosystems Engineering

journal homepage: www.elsevier.com/locate/issn/15375110

Research Paper

Understanding the microenvironment for dairy cows within an open Compost-Bedded Pack Barn in southeastern Brazil: Temporal and spatial behaviour during winter and summer

Carlos Eduardo Alves Oliveira [a,b], Ilda de Fátima Ferreira Tinôco [b], Túlio Souza Mariano [b], Fernanda Campos de Sousa [b], Rafaella Resende Andrade [c], Flávio Alves Damasceno [d], Gabriel Araújo e Silva Ferraz [d], Matteo Barbari [a,*]

[a] *Department of Agriculture, Food, Environment and Forestry, University of Florence, Florence, 50145, Italy*
[b] *Department of Agricultural Engineering, Federal University of Viçosa, Viçosa, Minas Gerais, 36570-900, Brazil*
[c] *Department of Biosystems Engineering, College of Agronomy, Federal University of Goiás, Goiânia, Goiás, 74690-900, Brazil*
[d] *Department of Engineering, Federal University of Lavras, Lavras, Minas Gerais, 37200-900, Brazil*

ARTICLE INFO

Keywords:
Animal thermal comfort
Dairy cattle
Embedded system
Housing systems
Monitoring
Modelling

ABSTRACT

Compost-Bedded Pack Barn (CBP) systems, predominantly built and operated in facilities with open sides, have been increasingly used worldwide. These facilities are more exposed to environmental fluctuations; therefore, real-time and spatial mapping of the thermal microenvironment is relevant, as it allows for the identification of areas and times with thermal comfort issues. In this context, the aim of this study was to characterise the temporal and spatial variation of thermal environmental variables (dry-bulb air temperature, relative humidity, and the Temperature–Humidity Index) within an open CBP system during winter and summer using a validated low-cost embedded system (LCES) developed for this purpose. The study was conducted in a typical CBP located in the Zona da Mata, an important dairy basin in Minas Gerais, Brazil's largest milk-producing region. The LCES was developed using low-cost electronic components, calibrated against reference instruments, and employed to monitor the microenvironment in a grid of points distributed throughout the Animal Occupied Zone during winter and summer. Based on temporal analyses, thermal conditions during winter were comfortable for lactating Holstein cows but were stressful in summer (9:10 a.m. to 6:30 p.m.), when there was potential for more efficient use of evaporative cooling (relative humidity $\leq$ 80.00%). Through spatial analyses, significant spatial variability in thermal conditions was observed, particularly in the morning and afternoon These findings suggest that adjustments to thermal protection systems in CBP facilities are necessary and provide a scientific basis for retrofitting existing facilities and designing new open CBP systems.

Nomenclature

3D	Three-Dimensional
A	Area, in m^2
a'	Practical range, in m
a	Range, in m
a.m.	Ante Meridiem
AC	Alternating Current
AFD	Airflow direction

(continued on next column)

(*continued*)

Afternoon	Mean values during the afternoon
AMBIAGRO	Research Centre on Ambience and Engineering of Agro-industrial Systems
AOZ	Animal Occupied Zone
APL	Aluminium Polyester Laminate
CBP	Compost-Bedded Pack Barn
CCE	Copper Clad Ethernet
CEUA	Animal Ethics Committee

(continued on next page)

This article is part of a special issue entitled: Technologies in Livestock published in Biosystems Engineering.
* Corresponding author.
E-mail addresses: eng.carloseaoliveira@gmail.com (C.E.A. Oliveira), iftinoco@ufv.br (I.F.F. Tinôco), tulio.mariano@ufv.br (T.S. Mariano), fernanda.sousa@ufv.br (F.C. Sousa), rafaella.andrade@ufg.br (R.R. Andrade), flavio.damasceno@ufla.br (F.A. Damasceno), gabriel.ferraz@ufla.br (G.A.S. Ferraz), matteo.barbari@unifi.it (M. Barbari).

https://doi.org/10.1016/j.biosystemseng.2026.104556
Received 24 April 2025; Received in revised form 19 July 2026; Accepted 21 July 2026
Available online 29 July 2026

(*continued*)

CV	Coefficient of variation, in %
Dawn	Mean values during the dawn
DC	Direct Current
DEA	Department of Agricultural Engineering
Exp	Exponential model
FDM	Fused Deposition Modelling
FS	Free Stall
Gau	Gaussian model
ICSP	In Circuit Serial Programming
I^2C	Inter Integrated Circuit
kg	Kilogram
LED	Light-Emitting Diode
LCD	Liquid Crystal Display
LCES	Low-cost embedded system
LDPE	Low-Density Polyethylene
IP	Ingress protection
m	Metres
Maximum	Absolute maximum values
ME	Mean-error
Minimum	Absolute minimum values
ML	Maximum Likelihood
Morning	Mean values during the morning
N	North
NaN	Not a Number
Night	Mean values during the night
NS	Not Specified
OLS	Ordinary Least Squares
PLA	Polylactic Acid
PWM	Pulse-Width Modulation
p.m.	Post Meridiem
REML	Restricted Maximum Likelihood
RH	Relative humidity, in %
RH_{Adj}	Relative humidity adjusted value, in %
RH_R	Relative humidity value read by the DHT22 sensor, in %
RTC	Real-Time Clock
S	South
s	Standard deviation
SD	Secure Digital
SDI	Spatial Dependence Index
SD_{ME}	Mean-error standard deviation
SD_{SE}	Standardised-error standard deviation
SE	Standardised error
Sph	Spherical model
T_{db}	Dry-bulb air temperature, in °C
$T_{db\text{-}Adj}$	Dry-bulb air temperature adjusted value, in °C
$T_{db\text{-}R}$	Dry-bulb air temperature value read by the DHT22 sensor, in °C
THI	Temperature-Humidity Index
UFV	Federal University of Viçosa
un	Unit
USB	Universal Serial Bus
US$	United States Dollar
UTCL	Upper Thermal Comfort Limit
W	West
WLS	Weighted Least Squares
$\wedge$	Minimum value
$\vee$	Maximum value
$C_0 + C_1$	Sill
C_0	Nugget effect
C_1	Contribution
$N(h)$	Number of experimental pairs $Z(X_i)$ and $Z(X_i + h)$
R^2	Coefficient of Determination
X_i	Record T_{db} or RH value measured by the DHT22 sensor module, in °C or %
$\overline{x}$	Mean value
Y_i	Adjusted T_{db} or RH value, in °C or %
$Z(X_i)$	Value at a sampled point
$Z(X_i + h)$	Value at a point displaced by a distance h
β_0	Intercept coefficient
β_1	Slope coefficient
$\hat{\gamma}(h)$	Estimated semivariance
ΔRH	Variation amplitudes of relative humidity, in %
ΔT_{db}	Variation amplitudes of dry-bulb air temperature, in °C
ΔTHI	Variation amplitudes of Temperature-Humidity Index

1. Introduction

In dairy systems where production cows are kept on pasture, there are recognised difficulties in meeting the animals' ambiance needs, particularly during periods of extreme thermal conditions, such as those observed in summer (Pons et al., 2023). Changes in environmental conditions can directly affect animal physiology and trigger thermal stress (Collier et al., 2019; Nordlund et al., 2019). Heat stress occurs more severely when animals are exposed to high air temperatures (T_{db}) for extended periods, accompanied by high relative humidity (RH). These are the two environmental variables with the greatest impact on thermal comfort (Cheng et al., 2024). Exposure of dairy cows to thermal stress conditions can result in reduced feed intake (Collier et al., 2019) and milk production (Gunn et al., 2019; Tao et al., 2020), impair fertility (Sammad et al., 2020) and increase the incidence of diseases such as mastitis and lameness (Dahl & McFadden, 2022).

Modern dairy farming has become increasingly intensive to minimise the impact of climatic fluctuations on milk productivity and consistency throughout the year, and to meet the growing and ongoing demand for dairy products (Bleizgys et al., 2022; Saitone & Sexton, 2017). Various confinement systems are used in intensive dairy production, with the Free Stall (FS) system being predominant (Mõtus et al., 2024). In this system, animals remain loose in facilities that include collective areas for movement, exercise and feeding, and individual areas for resting (stalls with bedding made from materials, such as rubber mats, sawdust, sand, or shredded rubber) (Bewley et al., 2017; Mõtus et al., 2024). However, in recent decades, the use of the Compost-Bedded Pack Barn (CBP) system has grown significantly worldwide, including in Brazil (Andrade et al., 2024; Blanco-Penedo et al., 2020; Guesine et al., 2023; Leso et al., 2020).

The CBP system is a model for housing dairy cattle in facilities with a collective bedding area composed of vegetable material (Leso et al., 2020; Llonch et al., 2020; Pons et al., 2023). Within CBP facilities, the vegetable material used for bedding, combined with the waste deposited by the animals in the collective resting area, is decomposed over time through composting processes. This is the main difference from other cattle confinement models that use bedding (Andrade et al., 2024; Biasato et al., 2019; Damasceno, 2020). According to numerous studies, the main advantages reported with the use of CBP systems on dairy farms include improvements in productivity, health, and longevity of lactating dairy cows, reductions in milk production costs, and better management of the waste generated by the animals (Bewley et al., 2017; Blanco-Penedo et al., 2020; Emanuelson et al., 2022; Leso et al., 2020).

Dairy cattle are typically housed in CBP systems within facilities presenting open sides. These facilities use active devices, such as fans or misters (the latter only in the feeding alley and activated only during the hottest periods of the day), to reduce the effects of thermal stress on the animals, renew the air, and maintain the composting process of the bedding (De Masi et al., 2021; Leso et al., 2020; Oliveira et al., 2023). Consequently, they are more exposed to external environmental fluctuations that occur throughout the day and year, due to each location's specific climatic and geographic conditions (Damasceno, 2020; De Masi et al., 2021; Pons et al., 2023). In addition to impacting animal thermal comfort, these climatic fluctuations can alter the dynamics of the bedding composting process and, as a result, affect the physical and chemical quality of the compost produced (Biasato et al., 2019; Leso et al., 2020; Llonch et al., 2020). Therefore, in addition to being important for managing animal thermal comfort, monitoring the thermal environment in such systems is crucial for ensuring proper management of the composting bedding (Andrade et al., 2022; Oliveira et al., 2022).

Although it is widely recognised that monitoring and, consequently, controlling the thermal environment in CBP systems are essential for ensuring productive efficiency, this is not the reality for many dairy farms. In practice, dairies often lack environmental control, or imprecise methods are used for monitoring the thermal environment, such as manual measurements and subjective observations. These practices are considered time-consuming, labour-intensive, and prone to human error (Arshad et al., 2022; Lee et al., 2024). Thus, to address the imposed environmental challenges, it is necessary to adequately monitor and characterise the thermal environment in the facilities over time, across the entire Animal Occupied Zone (AOZ), and under extreme climatic conditions, such as in winter and summer (Freitas et al., 2019; Leliveld et al., 2024). The results achieved in environmental characterisation studies of CBP systems under different climatic conditions are recognised as an important tool, as they can assist designers, technicians, and producers in managing and, consequently, ensuring the overall efficiency of the system (Andrade et al., 2022; Guesine et al., 2023; Oliveira et al., 2022). A detailed understanding of environmental challenges under extreme climatic conditions, as well as the spatial distribution of T_{db} and RH within the AOZ, enables the development of tailored solutions. These solutions can be adapted to different times of the day and seasons of the year. Therefore, improved management of the thermal environment can reduce energy consumption and contribute to more sustainable production.

Continuous monitoring of the thermal environment in animal facilities, including CBP systems, should be conducted using appropriate and purpose-specific data acquisition sensor networks (Li et al., 2024; Loukatos & Arvanitis, 2021). However, few companies specialise in the implementation of environmental monitoring systems for this type of facility, and when they do, the systems are often expensive and difficult to operate (Freitas et al., 2019). Thus, there is an urgent demand for the development and use of modern data acquisition systems based on Smart Livestock Farming. These systems should utilise low-cost sensors, actuators, and microprocessors and, when possible, integrate the Internet of Things and Big Data analysis (Arulmozhi et al., 2021; Kaur et al., 2023; Leliveld et al., 2024).

In addition to data acquisition through specialised environmental monitoring systems, data analysis is equally important and should be performed using appropriate and up-to-date statistical methods to accurately characterise thermal conditions over time and space. In this context, techniques, such as time series analysis and geostatistics, stand out. Time series analyses are essential for understanding the temporal dynamics of microclimatic variables within animal housing systems (Messeri et al., 2023; Mylostyvyi et al., 2020). Their use enables the identification of trends, daily and seasonal cycles, as well as anomalies that may negatively affect thermal comfort and the animals' productive and reproductive performance (Herrera-González et al., 2024). Spatial distribution analyses, on the other hand, are essential for identifying heterogeneity in thermal conditions throughout the area of animal production facilities (Garcia et al., 2023; Vieira et al., 2021). These analyses can be performed using geostatistical tools, which provide a robust framework for characterising spatial dependence. They also enable the generation of interpolated maps, and the identification of critical zones related to heat stress. This approach is widely validated and applicable to the spatial characterisation of microclimatic conditions in animal housing systems (Andrade et al., 2022; Ferraz et al., 2019; Guesine et al., 2023; Mota et al., 2019; Oliveira et al., 2022; Silva et al., 2023). Therefore, the integration of these two types of analyses represents a robust and indispensable methodological approach for a comprehensive and detailed assessment of the thermal environment in animal production systems.

It was hypothesised that the thermal microenvironment within open CBP systems exhibits marked temporal and spatial heterogeneity under contrasting seasonal conditions, leading to the occurrence of critical zones and periods that may compromise the thermal comfort of lactating dairy cows. Based on this hypothesis, the objective of this study was to characterise the temporal and spatial variation of the thermal environmental variables (T_{db}, RH, and THI) within an open CBP system during winter and summer using a validated low-cost embedded monitoring system. The proposed monitoring approach provides a practical framework for high-resolution assessment of the thermal environment in naturally ventilated dairy housing and supports evidence-based environmental management, the retrofitting of existing facilities, and the design of future CBP systems.

2. Material and methods

2.1. Characterisation of the compost-bedded pack barn (CBP) system and management of the thermal conditioning systems

This study was conducted under extreme climatic conditions (winter and summer) in a typical Brazilian CBP system with open sides, positive pressure mechanical ventilation, and water sprinkling in the feeding alley (activated only during the hottest times of the day). The CBP system was used for housing lactating dairy cows and was located on a commercial farm in the Zona da Mata region, Minas Gerais, Brazil (latitude 20°46′41″ S; longitude 42°48′51″ W; altitude 670 m). The local climate is classified as Cwa (mesothermal subtropical, with cold winters and hot, rainy summers), according to the Köppen-Geiger's classification (Monteiro & Martins, 2019). Based on long-term climatological normals (1981–2010), the region presents mean air temperatures ranging from approximately 18.00–20.00 °C in winter to 24.00–26.00 °C in summer. Relative humidity typically varies between 60.00 and 70.00% during the dry season and 75.00–85.00% in the rainy season, while annual precipitation ranges from 1200 to 1400 mm, with a marked concentration between October and March (Alvares et al., 2013; Fick & Hijmans, 2017; Sá Júnior et al., 2012), characterising a well-defined thermal and hydric seasonality.

The CBP system had its longitudinal axis oriented in the Southeast-Northwest direction and had the following construction characteristics: dimensions of 60.00 m in length, 27.60 m in width, and an eave height of 5.00 m (Fig. 1a and b). The roof was a gabled design with a metal structure and a covering, an open ridge with a 1.00 m overhang on the Southwest side, and lateral eaves extending 2.20 m (Fig. 1b). The floors in the service, drive-through, and feeding alleys were paved with textured concrete to prevent slips and had a longitudinal slope of 1% to facilitate waste drainage. To separate the bedding area from the feeding and service alleys, there were 0.20 m high small walls designed to prevent the transfer of bedding material and/or waste from one area to another. In the boundary area between the bedding zone and the feeding alley, there were also 1.20 m high masonry walls, positioned only where tipper drinkers' troughs were installed. They were intended to restrict animals' access to water directly from the bedding area.

The ventilation system consisted of six low-volume, high-speed axial fans operating under positive pressure: two three-blade fans (1.52 m diameter, 1.50 hp) with an airflow rate of 86,000 $m^3\,h^{-1}$ each, installed on the Southeast side, and four six-blade fans (1.53 m diameter, 2.00 hp) with an airflow rate of 55,000 $m^3\,h^{-1}$ each, installed in pairs along the longitudinal axis of the facility (at 12.00 and 36.00 m from the Southeast face). The fans were installed 3.00 m above the bedding level, inclined at 45° to the vertical, and operated continuously (24 h day^{-1}), promoting a predominant airflow direction (AFD) from Southeast to Northwest. The total ventilation rate was 392,000 $m^3\,h^{-1}$. Considering the internal volume of the building (8280 m^3), the corresponding air exchange rate was 47.30 h^{-1} (0.79 min^{-1}).

To promote the animals' body cooling, in addition to the mechanical ventilation, the CBP system was equipped with a 32.00 mm diameter water sprinkler line, positioned along the feeding line (Fig. 1a). The sprinkler line was installed 2.10 m above the feeding alley floor and was equipped with 29 low-pressure nozzles (flow rate of 2.00 L min^{-1}, 130° spray angle), spaced 2.00 m apart and angled at 45° relative to the vertical. The management of the water sprinkler system followed the practice already established on the commercial farm: it was activated for 1 min at regular 5-min intervals whenever the T_{db} exceeded 24.00 °C (setpoint).

For night-time illumination, the CBP system was equipped with eighteen 100 W LED lights, positioned 4.80 m above the bedding. The lights were evenly distributed throughout the facility (nine in the middle bedding area and nine at the boundary between the drive-through and the feeding alleys) and were switched on from 6:00 p.m. to 6:00 a.m.

The bedding material consisted of a heterogeneous mixture of

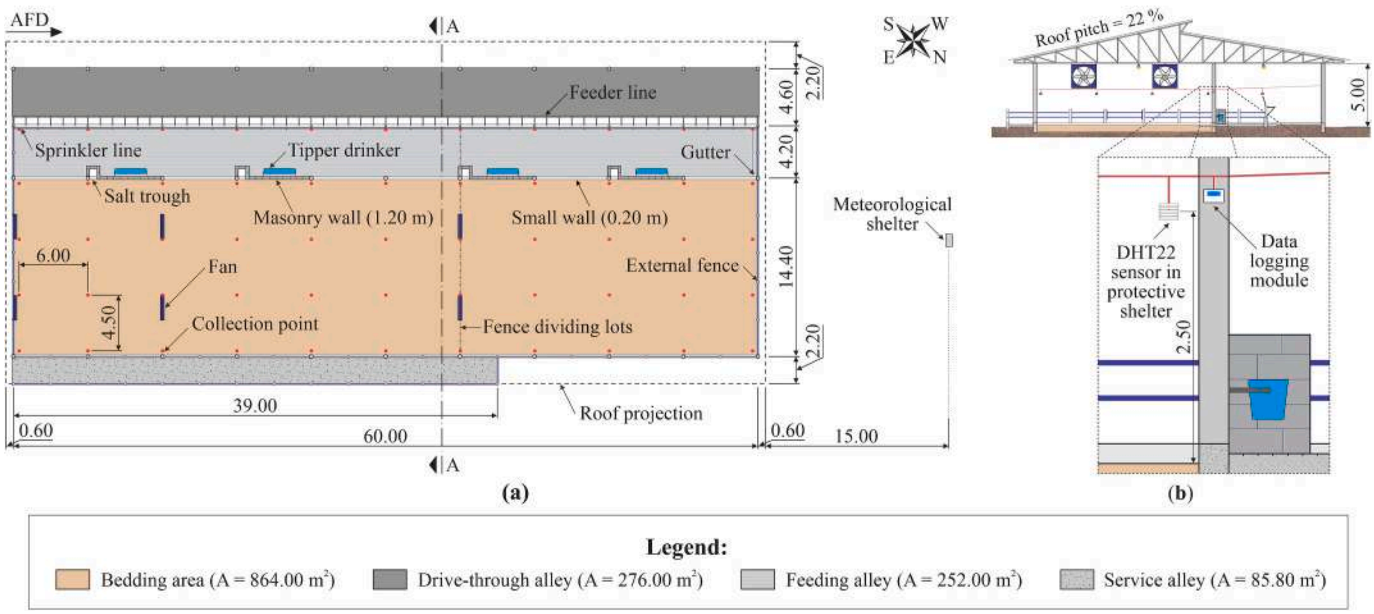

Fig. 1. Schematic representations of the Compost-Bedded Pack Barn system with open sides and positive pressure ventilation, showing **(a)** a floor plan with the arrangement of data collection points, and **(b)** cross-section AA, highlighting the positioning of the embedded system for thermal environment monitoring. A - area; AFD - airflow direction; N - north indication; dimensions in metres (m).

eucalyptus wood shavings and sawdust, with particle sizes of < 8.00 mm and between 8.00 and 25.00 mm, respectively, selected to ensure adequate porosity and support the activity of microorganisms within the composting matrix. The material used for the initial formation and subsequent replenishments presented moisture content ranging from 10.00 to 15.00%. The initial formation of the bedding pack was carried out through the addition of a 0.30 m thick layer of dry sawdust, corresponding to an estimated volume of 260.00 m^3, which, in combination with animal excreta (faeces and urine), initiated the composting process. At the beginning of the study (July), corresponding to the winter monitoring period, the bedding had been in use for approximately four months and presented a total depth of about 0.60 m, corresponding to an estimated volume of 520.00 m^3, resulting from the progressive accumulation of organic material, successive additions of dry bedding material, and the ongoing composting process.

Bedding management followed standard farm practices aimed at maintaining adequate moisture and aerobic conditions. Dry material (wood shavings and sawdust) was added whenever excessive moisture was identified, based on practical indicators, such as increased animal soiling, excessive compaction, or the occurrence of anaerobic conditions within the pack. The replenishment interval ranged from 12 to 15 days. During the winter monitoring period (July to August), two replenishments were performed, each consisting of approximately 20.00 m^3 of dry bedding material (≈8.00 tonnes per event). During the summer period (February to March), a single replenishment was carried out, with the addition of approximately 10.00 m^3 (≈4.00 tonnes) of dry material.

The bedding was mechanically turned twice daily (at 9:00 a.m. and 4:00 p.m.) using a tractor-mounted implement consisting of a combined rotary tiller and cultivator (working width of 2.00 m, five tynes, rotational speed of 540 rpm, maximum working depth of 0.50 m, and effective operating depth of approximately 0.30 m), ensuring aeration, homogenisation, and maintenance of aerobic conditions within the composting material.

All procedures involving animals were approved by the Animal Ethics Committee of the Federal University of Viçosa (CEUA/UFV; process n° 04/2021, approved on 16 May 2022; see Annex A). During the study, Holstein dairy cows in lactation (Purebred, average weight 600.00 kg) were housed in the CBP system. For each monitoring period, details on the number of animals housed, the bedding area available per animal, and daily milk production per animal are listed in Table 1 (milk productivity data extracted from the farm's milk control records).

The standard daily management routine for the cows housed in the CBP system was maintained, with dry matter being provided. The milking was carried out twice a day at 4:00 a.m. and 4:00 p.m., each lasting approximately 2.5 h. Milking operations were conducted in a 2 × 6 fishbone-type parlour machine, located in a facility adjacent to the CBP system. Water was provided *ad libitum* through four drinkers positioned in the feeding alley. This alley was cleaned once daily, in the morning, using a water discharge system in conjunction with manual scraping. The wastewater generated from cleaning the feeding alley was not reused.

2.2. Data acquisition and evaluation of the thermal environment in the compost-bedded pack barn (CBP) system

At the beginning of the study, an embedded system was developed and calibrated using low-cost and readily available electronic components. This phase was conducted at the Research Centre on Ambience and Engineering of Agro-industrial Systems of the Department of Agricultural Engineering, in the Federal University of Viçosa (AMBIAGRO/DEA/UFV). The list of electronic components and other materials used in the development of the embedded system for monitoring the thermal environment employed in this study, along with their respective quantities, technical specifications, and acquisition costs, is presented in Table 2.

As it was desirable for the embedded system to be modular and

Table 1
Information on the number of cows housed, bedding area available per animal, and daily milk production per animal in the Compost-Bedded Pack Barn system under study, during the experimental winter and summer periods.

Information	Experimental period	
	Winter	Summer
Number of animals housed (cows)	80.00	83.00
Available bedding area per animal (m^2)	10.80	10.68
Daily milk production per animal (kg day^{-1})	32.80 ± 13.35	31.12 ± 12.38

Table 2
List of electronic components and principal materials used in the development of the embedded system for monitoring the thermal environment employed in this study, including technical specifications, quantities, and unit costs.

Quantity	Component name	Technical specifications	Manufacturer	Price (US$) [a]	
				Unit	Total
11 un	Arduino Uno R3 Board	Microcontroller development board based on the ATmega328, featuring 14 digital input/output pins (6 with PWM), 6 analog inputs, 16 MHz oscillator, USB interface, DC power jack, ICSP header, and reset button. Operates at 5.00 V, suitable for embedded applications in data acquisition systems.	Atmel Corporation (San Jose, USA)	14.99	164.89
11 un	Data Logger Shield with RTC and SD Reader	Data logging module with SD card interface and DS1307 RTC, supporting FAT16/FAT32 file systems. Operates at 3.30 V, enabling timestamped data storage for monitoring and embedded system applications.	Dallas Semiconductor (Dallas, USA)	7.69	84.59
11 un	16 × 2 LCD Display	I^2C Blue Backlight LCD display with 16 × 2 character format, supporting 4-bit or 8-bit communication modes. Operates at a supply voltage of 5.00 V, enabling efficient data transfer and low power consumption. Ideal for embedded systems requiring a compact and clear visual interface for displaying information.	Shenzhen OMK Electronics Co. (Guangdong, China)	9.99	109.89
11 un	AC-DC adapter	Switched-mode power supply with 90–240 V AC input (50/60 Hz, 0.30 A maximum) and 5.00 V DC output (10.00 A maximum). Includes JP4 connector and built-in protection against short circuits and overheating. Operates in temperatures from 0 to 40 °C, suitable for embedded and automation systems.	Shenzhen Lianfeng Electronics (Shenzhen, China)	8.29	91.19
55 un	DHT22 sensor	Digital sensor model AM2302, capable of measuring temperature in the range of −40.00 to 80.00 °C with an accuracy of ± 0.50 °C, and relative humidity from 0 to 100 % with an accuracy of ± 2%. Designed for precise environmental monitoring in embedded systems and automation applications.	Aosong Electronics Co. (Guangzhou, China)	9.49	521.95
400 m	CCE 50 × 2 pairs cable	Electrolytic copper conductor with 0.50 mm diameter, APL shielding, and LDPE sheath. Provides signal integrity and durability for monitoring systems.	GP Cabos (São Paulo, Brazil)	0.32	128.00
1 kg	PLA translucent filament	1.75 mm diameter with ± 0.02 mm dimensional accuracy, supplied in a 1 kg spool. Suitable for FDM 3D printers, with recommended printing temperatures of 190–220 °C and bed temperature of 50–65 °C.	3D Lab Industry Ltda. (Belo Horizonte, Brazil)	15.99	15.99
NS	Other components	Cables, memory cards, pins, screws, silicone, etc.	NS	NS	133.50
				Total	**1250.00**

[a] Prices obtained in April 2025; 3D - Three-Dimensional; AC - Alternating Current; APL - Aluminium Polyester Laminate; CCE - Copper Clad Ethernet; DC - Direct Current; FDM - Fused Deposition Modelling; ICSP - In Circuit Serial Programming; I2C - Inter Integrated Circuit; LCD - Liquid Crystal Display; LDPE - Low-Density Polyethylene; NS - Not Specified; PLA - Polylactic Acid; PWM - Pulse-Width Modulation; RTC - Real-Time Clock; SD - Secure Digital; USB - Universal Serial Bus; and US$ - United States Dollar.

adaptable for monitoring thermal environments in animal housing with different characteristics, the development was carried out in the form of collection modules. Each collection module consisted of a data logging and display unit, which integrated an Arduino Uno R3, a Data Logger Shield with RTC and SD Reader, and a 16 × 2 LCD Display; and five DHT22 sensors, connected to the data logging and display unit by CCE 50 × 2 pairs of cables. A functional diagram of each collection module of the embedded system is illustrated in Fig. 2a.

The programming logic was developed in C++ using the Arduino Integrated Development Environment (IDE), an open-source software development platform. The C++ programming language was chosen for software development due to its status as a universal and high-level language, its compatibility with the microcontroller used for prototyping, and its compatibility with libraries that facilitated the handling of the hardware employed (Chang et al., 2020; Montironi et al., 2017).

For calibration, the system's collection modules and a commercial data logger sensor (HOBO®, model UX100-003; temperature range of −20.00 to 70.00 °C with an accuracy of 0.21 °C; relative humidity range of 0 to 100 % with an accuracy of 3.50 %; Onset Computer Corporation, Bourne, MA, USA) was used as the reference data logger for measuring temperature and humidity. The HOBO® UX100-003 data logger was used as the reference standard instrument for sensor calibration, due to its well-established accuracy and reliability in measuring T_{db} and RH under field conditions (Freitas et al., 2019). For 24 h, the values of T_{db} (°C) and RH (%) were recorded at regular intervals of 5 min. During this period, recorded values of T_{db} and RH were consistently numeric and accurate. Consequently, it was determined that the quality of the data obtained through monitoring with the embedded system in the CBP would not be compromised by NaN (Not a Number) reading errors, an issue that could arise with the use of low-cost sensors, potentially affecting the quality of the data and the overall environmental monitoring (Pramono et al., 2022).

The T_{db} and RH data obtained from the embedded system's sensor modules during validation were close to those recorded by the reference data logger. For greater reliability of the temperature and humidity data obtained through monitoring, it was understood that calibration curves

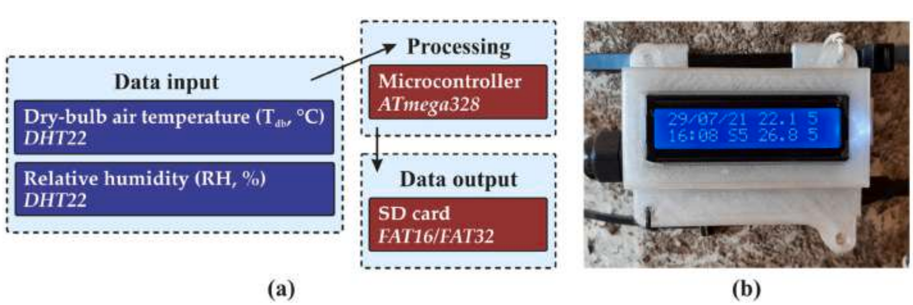

Fig. 2. **(a)** Schematic diagram of the operation of the low-cost embedded system and **(b)** capture of the data logging module during monitoring of dry-bulb air temperature (T_{db}, in °C) and relative humidity (RH, in %) inside the open Compost-Bedded Pack Barn system under study (indoor environment) and in the meteorological shelter (outdoor environment).

were necessary for each module, as the DHT22 is a capacitive sensor. To correlate the temperature and humidity values recorded by each DHT22 sensor module in the embedded system with those recorded by the data logger, calibration equations were obtained using linear regression, enabling the estimation of intercept (β_0) and slope (β_1) coefficients, as well as the coefficient of determination (R^2).

$$Y_i = \beta_1 \times X_i + \beta_0 \quad (1)$$

where: Y_i is the adjusted T_{db} or RH value; β_1 is the slope coefficient; X_i is T_{db} or RH value recorded by the DHT22 sensor module; β_0 is the intercept coefficient.

After calibration, the embedded system was used to monitor T_{db} and RH within the CBP system (Fig. 2b). Data acquisition of the thermal environment was carried out every 5 min, 24 h day^{-1}, for 15 consecutive days during winter (19 July to 2 August) and summer (28 February to 14 March). These periods were chosen for conducting the study as they typically represent the most challenging thermal conditions for managing the thermal environment and bedding in CBP systems. In the study area, high values of T_{db} are typically recorded, and precipitation occurs during the summer, conditions that can compromise the thermal comfort of lactating Holstein cows and increase the moisture content of the bedding material undergoing composting. In winter, low T_{db} values are typically recorded, which are desirable for the thermal comfort of the animals but not ideal for bedding management. This is because bacterial activity decreases, leading to increased bedding moisture, which results in greater soiling of the animals and a decline in milk quality. These monitoring periods were defined to capture representative intra-seasonal conditions under contrasting climatic scenarios; however, it was not intended to characterise interannual variability.

Data collection was carried out using a regular sampling grid composed of 55 equidistant points distributed across the AOZ, which included the bedding areas and the feeding alley. The use of regular sampling grids is recommended as it enhances statistical efficiency and facilitates field implementation (He et al., 2022; Wadoux et al., 2019), and it is widely applied in environmental studies of intensive animal production facilities. In such housing systems, which do not encompass large physical areas, it is broadly recognised that sample sizes below 100 points may be sufficient to detect meaningful spatial patterns (Andrade et al., 2022; Guesine et al., 2023; Oliveira et al., 2022; Silva et al., 2020).

The collection points were determined based on the structural characteristics of the CBP system, creating a rectangular grid (6.00 × 4.50 m) with 44 points located in the bedding area and 11 points in the feeding alley (see Fig. 1a). At each point in the grid, a DHT22 sensor module was installed, positioned 2.50 m above the bedding and the floor of the feeding alley, to allow for the passage of the tractor used for the daily turning of the bedding. According to the manufacturer, the DHT22 sensors do not have a specified ingress protection (IP) rating. Therefore, to protect the sensors from moisture, dust, and corrosive particles, each sensor module was housed in a protective shelter that did not affect the readings of T_{db} and RH.

Near the CBP system, a meteorological shelter was installed (see Fig. 1a), where data on T_{db} and RH were collected to characterise the external thermal conditions. In the meteorological shelter, data collection was conducted using a commercial data logger (HOBO®, model UX100-003). Similarly, external environmental data were collected every 5 min, 24 h day^{-1} during both monitoring periods.

The data on T_{db} and RH recorded during both monitoring periods (winter and summer) were used to calculate the THI, which represents the combined effect of these two climatic elements on the thermal comfort of the animals (Ji et al., 2020). The THI calculation was performed using Eq. (2), initially presented by Yousef (1985) and later described by Hahn (1995, 1999) and Mader et al. (2006):

$$THI = 0.81 \times T_{db} + (T_{db} - 14.40) \times \left(\frac{RH}{100}\right) + 46.40 \quad (2)$$

The classification of THI ranges specific to lactating Holstein cows was carried out as described by Hahn (1999), considering the following conditions: THI $\leq$74.00 = normal; 75.00 $\leq$ THI $\leq$78.00 = alert; 79.00 $\leq$ THI $\leq$83.00 = danger; THI $\geq$84.00 = emergency.

2.3. Statistical, geostatistical analyses, and mapping of the thermal environment in the compost-bedded pack barn (CBP) system

The data sets recorded during the monitoring periods of winter and summer were tabulated using Microsoft Excel®, v. 2406. Initially, the data collected continuously during each period were reviewed to identify potential errors or missing values. The measurements were obtained from sensors distributed throughout the AOZ of the CBP system (indoor environment) and from sensors placed in the meteorological shelter (outdoor environment). Subsequently, the T_{db} and RH values were adjusted using the calibration equations (Appendix A), and the absolute minimum, average, and absolute maximum values (obtained every 5 min) were calculated. Curves with the absolute minimum and maximum values of these variables were plotted to evaluate the temporal variation of T_{db} and RH over the 15 days of data collection for each period (winter and summer). In addition, average values with standard deviations for T_{db}, RH, and THI were calculated and used to plot daily behaviour curves for these variables both inside and outside the CBP system.

As the research also aimed to evaluate the spatial behaviour of the variables in the AOZ within the CBP system, the daily average data for T_{db}, RH, and THI were divided into four periods: dawn (00:00 a.m. to 05:59 a.m.), morning (06:00 a.m. to 11:59 a.m.), afternoon (00:00 p.m. to 05:59 p.m.), and night (06:00 p.m. to 11:59 p.m.). The temporal separation allowed the verification of the average spatial distribution of the data of interest in these four periods of the day. To characterise spatial patterns under extreme environmental conditions, the times at which the absolute minimum and maximum T_{db}, RH, and THI values occurred were identified. The corresponding datasets were then used to generate spatial distributions for winter and summer.

For all the datasets (mean values, by period; and point values, for times with extreme T_{db} and RH), minimum ($\wedge$), mean ($\bar{x}$), maximum ($\vee$), standard deviation (s), and coefficient of variation (CV) values were calculated using descriptive statistics. The CV was used to assess the dispersion of the data, following the classification suggested by Gomes (2000): CV < 0.10 = low dispersion; 0.10 ≤ CV < 0.20 = moderate dispersion; 0.20 ≤ CV < 0.30 = high dispersion; and CV ≥ 0.30 = very high dispersion.

The geostatistical methods were used to assess the spatial dependence and distribution of the variables of interest within the CBP system. The analyses were conducted using the R software environment, version 4.5.1 (R Core Team, 2024), with the geoR package, version 1.9-6 (Ribeiro Júnior & Diggle, 2001; Ribeiro. et al., 2025). Experimental variograms were fitted to analyse the spatial dependence of the variables. The variograms were obtained using the classical estimator (Matheron, 1962), as expressed in Eq. (3):

$$\hat{\gamma}(h) = \frac{1}{2N(h)} \sum_{i=1}^{N(h)} [Z(X_i) - Z(X_i + h)]^2 \quad (3)$$

where: $\hat{\gamma}(h)$ is the estimated semivariance; N(h) is the number of experimental pairs $Z(X_i)$ and $Z(X_i + h)$; $Z(X_i)$ is the value at a sampled point; and $Z(X_i + h)$ is the value at a point displaced by a distance h.

Prior to variogram modelling, an exploratory data analysis was performed to assess the statistical behaviour of the variables, including descriptive statistics, normality testing using the Shapiro–Wilk test, and graphical inspection of spatial distribution. Although normality was assessed, no data transformation or detrending procedure was applied because geostatistical methods do not require strict normality and the original observations were preserved. Given the relatively small spatial extent of the study area and the regular sampling grid adopted, the intrinsic stationarity assumption was considered acceptable for variogram estimation and spatial modelling, as commonly adopted in studies involving thermal environment mapping and geostatistical analysis in animal production systems, particularly in confined housing conditions with similar spatial scales (Andrade et al., 2022; Guesine et al., 2023; Oliveira et al., 2022; Silva et al., 2020). This approach is consistent with the theoretical framework of geostatistics, in which spatial dependence is primarily governed by the separation distance between observations when large-scale trends are absent.

Estimating the semivariogram function is not a trivial task, as different strategies, based on distinct principles and assumptions, many of which are difficult to verify, can be adopted and statistically justified (Mingoti & Rosa, 2008). Given the methodological diversity involved in semivariogram estimation, this study combined different statistical methods and models in order to achieve fits that adequately represent the field conditions: (i) four different methods were tested, namely Ordinary Least Squares (OLS), Weighted Least Squares (WLS), Maximum Likelihood (ML), and Restricted Maximum Likelihood (REML); (ii) in conjunction with these methods, the traditional Spherical (Sph), Exponential (Exp), and Gaussian (Gau) models were fitted (McBratney & Webster, 1986; Vieira et al., 2010) for evaluation. A total of twelve model-fitting combinations were tested: OLS-Sph, WLS-Sph, ML-Sph, REML-Sph, OLS-Exp, WLS-Exp, ML-Exp, REML-Exp, OLS-Gau, WLS-Gau, ML-Gau, and REML-Gau.

To assess the quality of the adjustments obtained by combining the four estimation methods with the three theoretical models, cross-validation procedures were employed, which are widely recognised as an appropriate approach for selecting semivariogram models (Ferraz et al., 2019; Johann et al., 2010; Silva et al., 2021). Cross-validation was performed by sequentially removing each observation and estimating it via ordinary kriging using the remaining samples (Isaaks & Srivastava, 1989; Kerry & Oliver, 2007). The evaluation of model performance was based primarily on cross-validation statistics, including mean error (ME), standardised error (SE), mean-error standard deviation (SD_{ME}) and standardised-error standard deviation (SD_{SE}). In addition, complementary criteria were considered to ensure consistency and robustness of the selected model. These included the analysis of standardised errors, with preference for models presenting no significant deviation from normality (Shapiro–Wilk test), and the regression between observed and predicted values, in which the intercept should be close to zero, the slope close to one, and R^2 as high as possible. Finally, the structural behaviour of the experimental semivariogram was also evaluated, including the magnitude of the nugget effect, the coherence of semivariance values along the distance classes, and the stability of the semivariogram at the sill, with values consistent with the sample variance. The final selection of the semivariogram model was based on the joint evaluation of these criteria, prioritising models that provided both statistically consistent predictions and a physically meaningful representation of spatial dependence.

The relationship between sample variance and semivariogram sill was also analysed as a consistency check. When the experimental semivariogram exhibited a well-defined sill, this value was expected to be close to the sample variance (Webster & Oliver, 2007). Semivariograms with a sill not only satisfy the intrinsic hypothesis but also meet the second-order stationarity assumption. Under this assumption, the variance of the studied variable can be estimated both by the sample variance and by the sill of the fitted semivariogram (Ferraz et al., 2014).

For the identified best variogram models, the theoretical model coefficients for the variogram were extracted, namely: nugget effect (C_0), contribution (C_1), sill ($C_0 + C_1$), range (a), and practical range (a'). Spatial dependence analyses for each variable were conducted using the Spatial Dependence Index [$SDI = C_0/(C_0 + C_1)$], with $SDI \leq 0.25$ = strong spatial dependence, $0.25 < SDI \leq 0.75$ = moderate spatial dependence, and $SDI > 0.75$ = weak spatial dependence (Cambardella et al., 1994).

To estimate values at unsampled locations within the CBP system, ordinary kriging was applied to generate spatial distribution maps using ArcGIS® v. 10.4 (Esri, Redlands, CA, USA), with the Spatial Analyst and Geostatistical Analyst extensions (Oliveira et al., 2024).

3. Results and discussion

3.1. Embedded system developed, data acquisition and adjustment

The embedded system developed in this study was designed with modular architecture, comprising independent data collection units, which allows for its adaptation to various structural layouts of animal production facilities. The versatility of this system is regarded as one of its main advantages, making it suitable for spatial and temporal monitoring of thermal environments under varying climatic and architectural conditions. This feature was supported by Arulmozhi et al. (2021) and Kaur et al. (2023), who emphasised the importance of modularity and scalability in systems applied to precision livestock farming. The integration of low-cost sensors, microcontrollers, and storage modules aligned with the principles recommended by Leliveld et al. (2024), who emphasised the need for developing and implementing open-source, reprogrammable, and easily maintainable monitoring systems for use in animal production facilities.

To assess the technical feasibility of the embedded system developed, the T_{db} and RH values recorded by the DHT22 sensors integrated into the system were compared with those measured by reference data loggers (HOBO®, model UX100-003) using calibration equations (Appendix A). Fig. 3 shows the calibration curves obtained for T_{db} and RH for one position (no. 1) with good agreement between the values of T_{db} and RH (R^2 of ~0.98 and ~0.97, respectively). Calibration equations and R^2 values for the remaining sensor positions are provided in Appendix A (Table A1). For T_{db}, excellent agreement was observed between the values recorded by the embedded system's sensor modules and the standard reference sensor ($0.97 < R^2 < 0.99$). For RH, good agreement was observed between the recorded and reference values ($0.92 < R^2 < 0.99$). Overall, the calibration models presented intercept (β_0) values close to zero and slope (β_1) values close to unity, demonstrating minimal systematic bias. The R^2 values were consistently high, with mean values > 0.97 for T_{db} and >0.92 for RH, indicating that this type of low-cost sensor provided reliable measurements, in agreement with Freitas et al. (2019) and Pramono et al. (2022). Thus, it can be inferred that the embedded system developed was suitable for monitoring real production environments in animal housing facilities, enabling the acquisition of reliable data from multiple points within the areas of interest.

From an economic perspective, the total cost for assembling 11 data collection modules, comprising 11 data logging and display units with 55 DHT22 sensors distributed across the area of interest was approximately US$1250.00 (Table 2). Accordingly, each monitoring point, including all associated infrastructure (Arduino, shield, display, power supply, cabling, etc.), had an average cost of ~US$22.73. By comparison, a single commercial data logger of the HOBO® UX100-003 type had an estimated market price of US$150.00, according to the Onset Computer Corporation (price checked in April 2025). Therefore, to equip 55 monitoring points as used in this study, an investment of approximately US$8250.00 would be required with commercial sensors, representing an increase of ~560.00% in the total cost. The embedded system developed was an economically viable alternative, especially for applications requiring a high sensor density for detailed spatial monitoring. The use of open platforms also reduced software licensing costs and facilitates future updates, the lifespan of the embedded system developed (Chang et al., 2020; Montironi et al., 2017).

From a cost-benefit perspective of the thermal-environmental data obtained, it is also important to highlight that the embedded system developed enabled continuous data acquisition. Continuous acquisition of thermal-environmental data with high temporal and spatial frequency is essential for identifying critical thermal zones to enable the

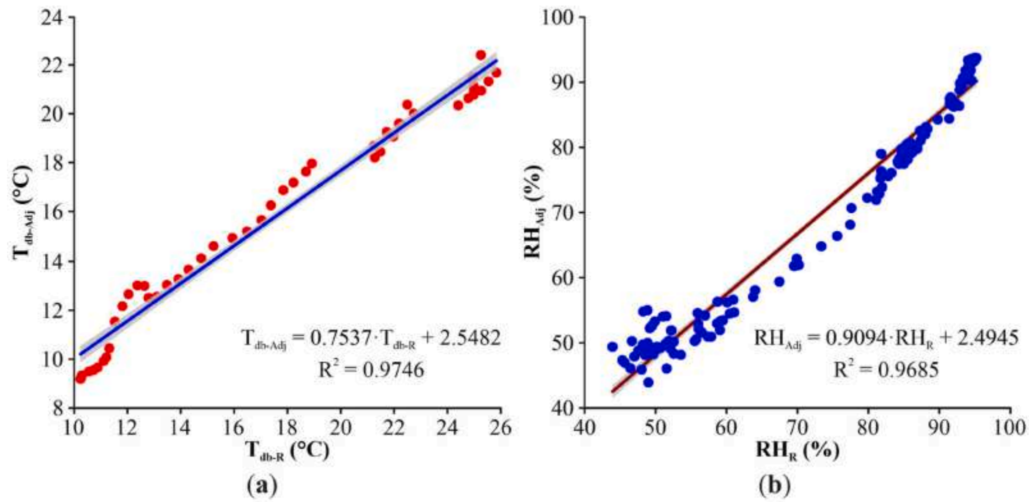

Fig. 3. Calibration curves of **(a)** dry-bulb air temperature (T_{db}, in °C) and **(b)** relative humidity (RH, in %), for the DHT22 sensor n° 1, which was part of the low-cost embedded system for monitoring the thermal environment, compared to the standard recording sensor. T_{db-Adj} - dry-bulb air temperature adjusted value; T_{db-R} - dry-bulb air temperature value read by the DHT22 sensor; RH_{Adj} - relative humidity adjusted value; RH_R - relative humidity value read by the DHT22 sensor.

optimisation of cooling systems (ventilation, sprinkling, etc.) and improvement of animal welfare and productive efficiency (Arshad et al., 2022; Lee et al., 2024).

Regarding the technical knowledge required for the implementation and maintenance of the developed embedded system, it can be considered intermediate, requiring basic knowledge in electronics and programming. However, it is important to highlight that this challenge can be mitigated through partnerships with educational and research institutions, technical training, and the use of tutorials available on open-source platforms. In addition, the formation of local technical assistance networks can promote the widespread adoption of low-cost embedded technologies in the dairy sector (Loukatos & Arvanitis, 2021).

Overall, the developed and validated embedded system had a significantly lower cost than equivalent commercial solutions, without compromising data reliability. It represented a technically viable solution for producers and researchers interested in environmental monitoring of animal production facilities with the potential to strengthen sustainable practices aligned with the principles of precision livestock farming.

3.2. Temporal analyses of variables and thermal-environmental index in the compost-bedded pack barn (CBP) system

The continuous collection of T_{db} (in °C) and RH (in %) during the winter and summer periods resulted in 4319 pairs of T_{db} and RH data for each CBP monitoring point and the shelter, totalling 241,864 pairs for each monitoring period. These datasets were adjusted and used in temporal and spatial analyses of the variables and thermal environment

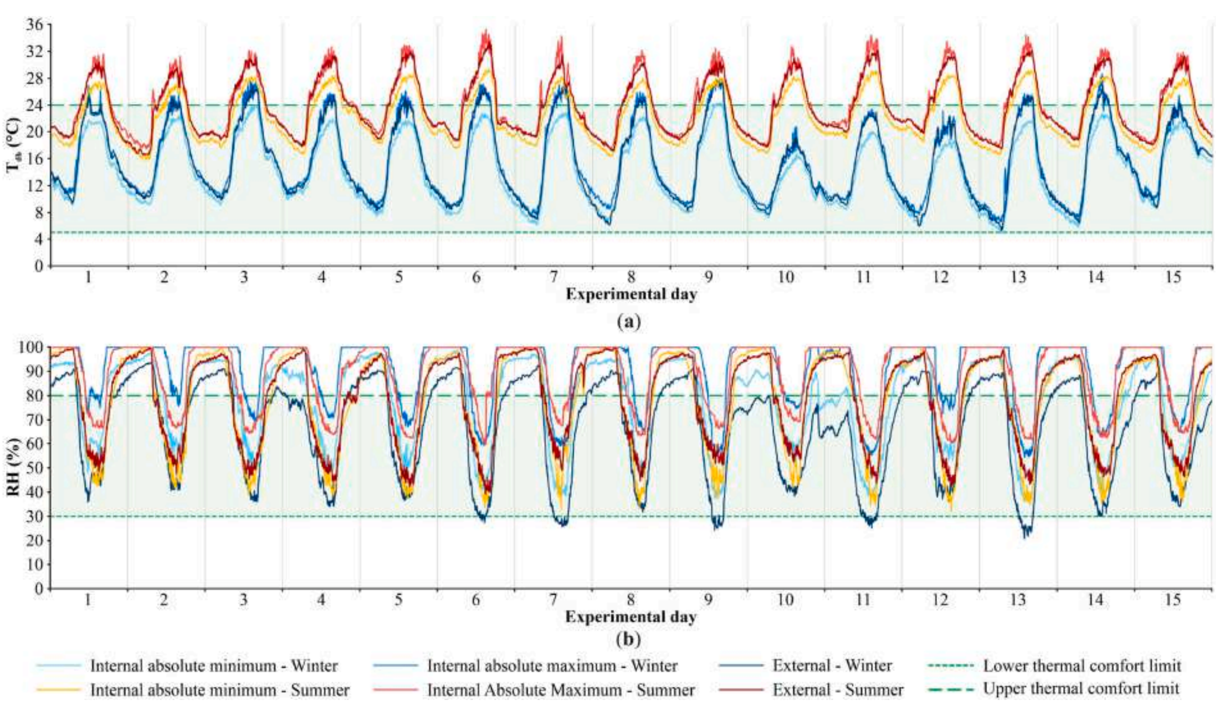

Fig. 4. Curves of absolute minimum and maximum values of **(a)** dry-bulb air temperature (T_{db}, in °C) and **(b)** relative humidity (RH, in %), inside and outside the Compost-Bedded Pack Barn system under study, during the experimental periods of winter and summer.

index. Fig. 4 illustrates curves showing the absolute minimum and maximum values of T_{db} and RH, both inside the CBP system and for these climatic elements in the external environment, during both monitoring periods. During winter and summer, similar variations of T_{db} were observed in both the internal and external environments of the CBP system (Fig. 4a). Since this was a CBP system with open sides, this was expected, as there was a high correlation between the internal and external T_{db} conditions (Endres et al., 2011).

Although the curves representing the internal and external T_{db} values over the winter and summer periods were close to each other, the absolute maximum values of T_{db} inside the CBP system were consistently higher than those recorded in the external environment (Fig. 4a). These findings are consistent with those reported by Andrade et al. (2022). However, the temporal analysis of absolute maximum T_{db} values alone was insufficient to conclude that the environmental conditions within the CBP system were more thermally challenging than those in the external environment, as these values may have been restricted to specific areas within the AOZ and therefore may not have been representative of the entire occupied zone.

In winter, the absolute minimum T_{db} record was 4.73 °C (on day 13 at 6:25 a.m.), whereas in summer it was 15.84 °C (on day 2 at 4:00 a.m.) (Fig. 4a). Considering that T_{db} remained below the lower critical comfort limit for lactating Holstein dairy cows (5 °C according to Nääs, 1989), for <15 min, it can be inferred that the recorded absolute minimum values did not constitute significant cold stress.

On the other hand, T_{db} values > 24 °C, the Upper Thermal Comfort Limit (UTCL) for European dairy cattle according to Nääs (1989), were recorded on 12 days during winter and on all 15 days during summer (Fig. 4a). During winter, a season typically associated with milder climatic conditions (Monteiro & Martins, 2019), T_{db} peaks of up to 3.00 °C above the UTCL were recorded. These results indicate that even during the cold season, the thermal conditions within the CBP system occasionally exceeded the UTCL for lactating Holstein dairy cows.

In summer, absolute maximum T_{db} values were consistently >30 °C (Fig. 4a). During this period, the most critical thermal conditions for the dairy cows housed in the CBP system were observed on the 6th, 7th, 11th and 13th days, when T_{db} peaks were recorded at > 10 °C above the UTCL (35.23 °C, 34.24 °C, 34.37 °C, and 34.40 °C, respectively). In such conditions, the physiological and behavioural mechanisms responsible for regulating core body temperature become insufficient to maintain thermal homeostasis, resulting in heat stress (Nordlund et al., 2019). This condition has several adverse consequences, such as reduced feed intake (Collier et al., 2019), decreased milk production (Gunn et al., 2019; Tao et al., 2020) and impaired reproductive performance (Sammad et al., 2020). Since the average daily milk production per animal in summer was numerically lower than in winter (32.80 ± 13.35 and 31.12 ± 12.38 kg animal^{-1} day^{-1}, respectively; Table 1), this difference may be partly associated with the thermal conditions recorded, which were more thermally challenging for the animals.

The temporal variation in both minimum and maximum RH values inside and outside the CBP system was similar throughout the monitored periods, despite some lower values being recorded outside during winter (RH ≤ 30 %; Fig. 4b). Such results were anticipated for the outdoor environment of the CBP during winter, as this season is typically cold and dry in areas with a Cwa climate, influenced by local convective processes and South American monsoons (Monteiro & Martins, 2019).

Inside the CBP system, the absolute maximum values of RH remained higher than those recorded outside, always exceeding 30 %, and reached saturation at night on all monitored days, both in winter and summer (Fig. 4b). During daylight hours, there was a tendency for RH values to be >50 % inside the CBP system. This can be attributed to the increase in RH due to the composting process of bedding, evaporation and spillage from the tipper drinkers, animal respiration, and the presence of animal waste (Oliveira et al., 2022).

Between 6:00 p.m. and 8:00 a.m., there was a tendency for RH values inside the CBP system to remain above the recommended range for optimal thermal exchange in animals (30-80%, according to Nääs, 1989) (Fig. 4b). In this case, it can be inferred that the consistently high RH values observed during both winter and summer was associated with the external environmental conditions at the location. Persistently high RH values can lead to increased health issues in animals (such as bronchitis, pneumonia, mastitis, etc.) and can raise the moisture levels in the bedding, resulting in dirtier cows and a subsequent decline in milk quality (Eckelkamp et al., 2016; Leso et al., 2020). Therefore, consistently high RH values inside animal housing are undesirable from a management perspective and should be addressed through appropriate ventilation and environmental control strategies.

When high RH values coincided with elevated T_{db}, as observed on certain days and times during summer (Fig. 4a and b), thermal exchanges may be compromised, thereby affecting thermal comfort. When RH is high, the vapor pressure gradient decreases, which reduces evaporative heat loss (such as sweating and panting) (Herbut et al., 2018). Therefore, when combined with a high T_{db}, which reduces the thermal gradient between the core body temperature and the surrounding ambient temperature, elevated RH values impair heat dissipation and lead to heat stress in animals (Collier et al., 2019). Heat stress caused by the prolonged exposure of dairy cows to simultaneously high T_{db} and RH can reduce feed intake and milk production, impair fertility, and increase the incidence of diseases such as mastitis and lameness (Dahl & McFadden, 2022).

To analyse the hourly variation of T_{db}, RH and THI inside and outside the CBP system, the graphs illustrated in Fig. 5 were generated. In both winter and summer, the average T_{db} inside the CBP system was lower than that recorded outside, particularly between 9:00 a.m. and 5:00 p.m., when the average temperature difference between the internal and external environments exceeded 1.50 °C (Fig. 5a). The lower average T_{db} observed inside the CBP system compared to the external environment was anticipated, as the presence of a metallic cover in the CBP system, which has high thermal emissivity and reflectance, can reduce the incident solar radiation load by up to 30.00 %, thereby decreasing the average internal T_{db} (Kolokotroni et al., 2018).

The reduction in average T_{db} during periods of solar radiation was present can also be partly explained by the operation of mechanical ventilation in the bedding area of the CBP system, which facilitates air movement, enhances thermal exchanges, and consequently lowers the T_{db} (Mrema et al., 2011; Oliveira et al., 2022). Additionally, this may also be related to the water sprinkling in the feeding alley (only during the hottest times of the day), a process implemented to promote the cooling of the animal's body.

Despite the lower average T_{db} values recorded inside the CBP system compared with the external environment, the average T_{db} remained above 24.00 °C from 9:10 a.m. to 6:30 p.m. (Fig. 5a). During this period, the environmental conditions were considered thermally stressful for lactating Holstein cows. In such situations, dairy cattle tend to spend more time standing than resting, a condition that, although an adaptive response to heat stress, adversely affects animal welfare and productivity (Allen et al., 2015; Reuscher et al., 2023).

During the period when T_{db} ≥ remained 24.00 °C, the RH inside the CBP ranged from 56.12 ± 5.78 % (2:55 p.m.) to 84.46 ± 5.88 % (6:30 p.m.), with values predominantly < 80.00 % (Fig. 5b). These conditions indicated the potential for exploring animal body cooling and/or air evaporative cooling (through latent heat) in the CBP system during the hottest times of the day.

In this type of confinement system, animal body cooling can be achieved using water sprinkler systems, with droplets ranging from 15.00 to 50.00 μm in diameter, to wet the animals' skin (Fournel et al., 2017; Polsky & von Keyserlingk, 2017). However, this method should only be used in the feeding alley area to avoid wetting the bedding and must be combined with mechanical ventilation systems. These systems are essential to generate airflow over the animals, facilitate water evaporation, and ensure the expected body cooling of the housed dairy cows (Arcidiacono, 2018; Renaudeau et al., 2012).

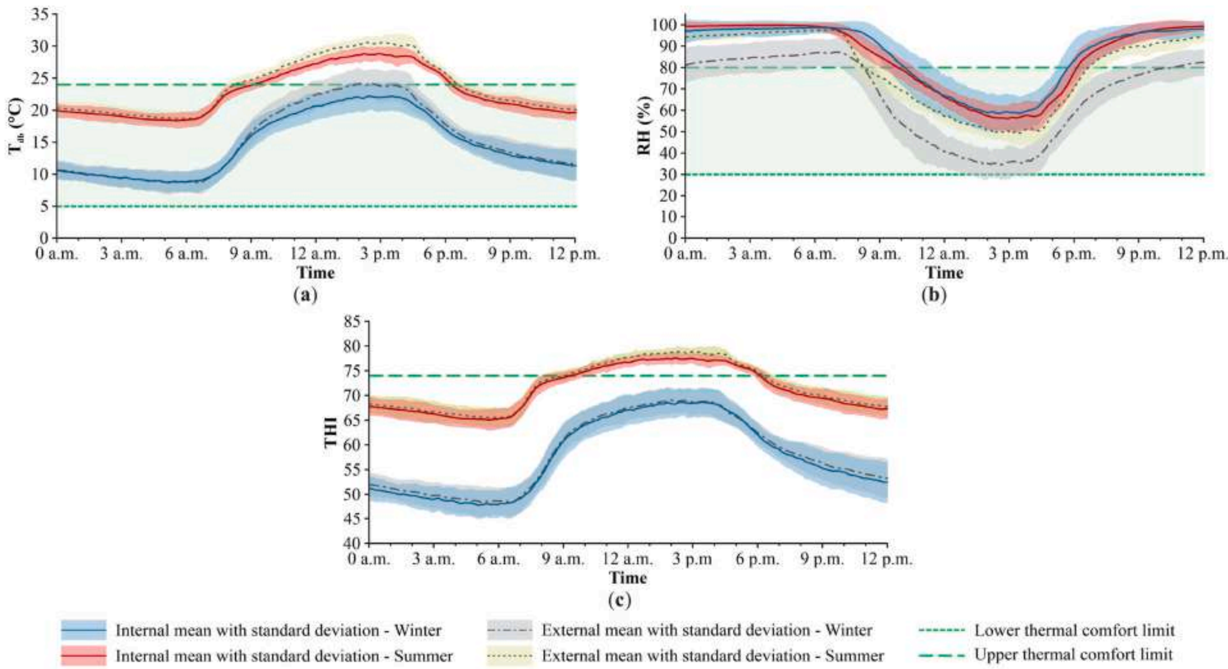

Fig. 5. Curves of mean values, with standard deviation, for **(a)** dry-bulb air temperature (T_{db}, in °C), **(b)** relative humidity (RH, in %), and **(c)** Temperature-Humidity Index (THI), internal and external to the Compost-Bedded Pack Barn system under study, during the experimental winter and summer periods.

Indoor thermal conditions can also be improved using evaporative air-cooling systems. In this case, water misting systems (installed only in the feeding alley) combined with positive-pressure mechanical ventilation can be used. Alternatively, evaporative padding systems combined with negative-pressure mechanical ventilation can be employed, but these are recommended only for fully enclosed CBP systems (Andrade et al., 2024; De Masi et al., 2021). In both cases, the use of mechanical ventilation is mandatory, and the reduction in T_{db} occurs only when there is a change in the water content of the air and some of the energy (heat) is consumed to evaporate the water (Mrema et al., 2011; Smith et al., 2016).

Regarding body cooling through water sprinkling in the feeding alley, it is worth noting that the CBP system under study was already equipped with this system, which was activated when $T_{db} \geq 24.00\,°C$ (for 1 min at 5-min intervals). During the monitoring period, it was observed that the water sprinkling system was only activated in summer when temperatures were predominantly higher than the setpoint used (Fig. 5a). This suggested that the placement of the sensor used to activate the sprinkling system was inadequate, as $T_{db} \geq 24.00\,°C$ was recorded in some areas of the CBP system even during winter.

Given the persistently high temperatures recorded during the summer (Fig. 5a), improvements are needed in the thermal protection systems used in the CBP system. For example, installing mechanical ventilation lines in the feed alley would enhance the evaporation of water sprayed on the animals' skin and the flooring, thereby maximising both body and air cooling. Additional strategies to improving environmental thermal conditioning could also be explored. Increasing the overall ventilation rate across the entire positive-pressure mechanical ventilation system, using evaporative cellulose pads combined with negative-pressure mechanical ventilation (which would involve a complete redesign of the CBP system), or enhancing the building's thermal insulation (such as spraying water on the roof or using insulating barriers) are potential options. Nonetheless, it is essential to understand the distribution of T_{db}, RH and THI within the CBP system to make specific and effective decisions that are viable and sustainable from technical, economic, energy, and social perspectives.

Temperature is the most significant component in the determination of THI (Ji et al., 2020; Tao et al., 2020), and the combined effect of T_{db} and RH resulted in THI values showing a daily pattern similar to that of T_{db} (Fig. 5c). Despite similar patterns, it was observed that the THI curves during winter and summer exhibited a greater flattening during the hottest part of the day, from 9:10 a.m. to 6:30 p.m. (Fig. 5c), when compared to those of T_{db}. Since the lowest average RH values were recorded during this time interval, it is inferred that the process of thermal exchange through latent pathways (sweating and panting) was enhanced, resulting in the observed outcomes.

During winter, the average THI values throughout the day ranged from 47.82 ± 2.78 (5:05 a.m.) to 68.63 ± 2.55 (2:30 p.m.), remaining below the heat stress threshold (THI $<$ 74.00). This suggested that the thermal conditions within the CBP system under study were comfortable for lactating Holstein dairy cows (Fig. 5c). During summer, although the THI range was narrower (around 12.50) compared to winter, higher average hourly values were observed, ranging from 65.07 ± 2.04 (5:30 a.m.) to 77.61 ± 1.08 (2:10 p.m.) (Fig. 5c). In Summer, the most challenging conditions for lactating cows were observed between 9:20 a.m. and 6:05 p.m., when the THI was $\geq$ 74.00. These conditions suggest that the Holstein dairy cows in lactation may have undergone physiological and behavioural adjustments during the day, such as reduced feed intake (Collier et al., 2019) and decreased resting time (Nordlund et al., 2019), which may have contributed to the lower average daily milk production observed during summer (Table 1).

The monitoring campaigns were conducted that the monitoring campaigns were conducted over 15 consecutive days in each season, which provided a detailed characterisation of intra-seasonal thermal patterns under contrasting climatic conditions. However, this temporal window does not capture inter-annual variability. Therefore, the present results should be interpreted as representative of the specific climatic conditions observed during the monitoring periods, while providing valuable insights into the temporal variation of the thermal environment within the CBP system.

3.3. Spatial analyses of variables and the thermal-environmental index in the compost-bedded pack barn (CBP) system

To characterise the spatial distribution and variability of the environmental variables throughout the CBP system, geostatistical

Table 3
Methods, models, and parameters obtained from the semivariograms fitted for dry-bulb air temperature (T_{db}), relative humidity (RH), and Temperature-Humidity Index (THI), inside a lactating cow accommodation in an open Compost-Bedded Pack Barn system under study, during winter and summer periods in Brazil.

Variable	Period	Method	Model	C_0	C_1	$C_0 + C_1$	*a*	*a′*	SDI	ME	SD_{ME}	SE	SD_{SE}
$T_{db\text{-}Dawn}$	Winter	OLS	Spherical	0.0048	0.0548	0.0596	5.5792	5.5792	0.0813	0.0000	0.2389	0.0000	0.9721
	Summer	OLS	Spherical	0.0035	0.0417	0.0452	5.5295	5.5295	0.0772	0.0000	0.2138	0.0000	0.9991
$T_{db\text{-}Morning}$	Winter	OLS	Spherical	0.0073	0.0760	0.0833	5.3792	5.3792	0.0875	0.0000	0.2885	0.0000	0.9922
	Summer	OLS	Spherical	0.0105	0.0919	0.1024	6.3129	6.3129	0.1024	0.0007	0.3140	0.0011	0.9798
$T_{db\text{-}Afternoon}$	Winter	OLS	Spherical	0.0129	0.1681	0.1810	5.4192	5.4192	0.0714	0.0000	0.4242	0.0001	0.9896
	Summer	REML	Spherical	0.0017	0.3266	0.3283	31.0624	31.0624	0.0053	0.0058	0.2697	0.0102	0.9922
$T_{db\text{-}Night}$	Winter	OLS	Spherical	0.0032	0.0606	0.0638	5.3292	5.3292	0.0501	0.0000	0.2471	0.0000	0.9707
	Summer	REML	Spherical	0.0042	0.0407	0.0449	5.9109	5.9109	0.0933	0.0001	0.2089	0.0002	0.9815
$T_{db\text{-}Minimum}$	Winter	WLS	Spherical	0.0078	0.2003	0.2082	5.8728	5.8728	0.0377	0.0003	0.4461	0.0003	0.9734
	Summer	OLS	Spherical	0.0092	0.1339	0.1430	5.4110	5.4110	0.0641	−0.0001	0.3736	−0.0002	0.9805
$T_{db\text{-}Maximum}$	Winter	ML	Spherical	0.0960	1.3710	1.4670	41.7207	41.7207	0.0654	0.0215	0.6157	0.0174	0.9730
	Summer	REML	Gaussian	0.0850	2.6230	2.7080	10.5300	18.2312	0.0314	0.0113	0.4924	0.0097	0.9833
RH_{Dawn}	Winter	WLS	Spherical	0.1528	1.6724	1.8252	6.0645	6.0645	0.0837	−0.0007	1.3478	−0.0003	0.9949
	Summer	REML	Spherical	0.0095	0.1383	0.1478	8.0372	8.0372	0.0643	0.0011	0.3639	0.0015	0.9998
$RH_{Morning}$	Winter	WLS	Spherical	0.4495	4.7484	5.1979	5.5298	5.5298	0.0865	−0.0006	2.2960	−0.0001	1.0000
	Summer	OLS	Spherical	0.0695	3.0338	3.1033	8.6764	8.6764	0.0224	0.0012	1.6125	0.0004	0.9996
$RH_{Afternoon}$	Winter	WLS	Spherical	0.8395	9.6707	10.5103	5.6319	5.6319	0.0799	−0.0018	3.2218	−0.0003	0.9874
	Summer	REML	Gaussian	1.3598	11.3500	12.7098	6.5210	11.2857	0.1070	−0.0155	2.2947	−0.0033	0.9987
RH_{Night}	Winter	WLS	Spherical	0.4395	4.8793	5.3188	5.2918	5.2918	0.0826	−0.0002	2.3223	0.0000	0.9989
	Summer	OLS	Spherical	0.1595	1.8776	2.0371	5.7533	5.7533	0.0783	0.0010	1.4340	0.0003	0.9998
$RH_{Minimum}$	Winter	WLS	Spherical	1.4972	16.2998	17.7969	5.4593	5.4593	0.0841	−0.0007	3.1586	−0.0001	0.9785
	Summer	OLS	Spherical	2.0498	24.8757	26.9256	5.5467	5.5467	0.0761	−0.0002	2.9684	0.0000	0.9803
$RH_{Maximum}$	Winter	OLS	Spherical	0.1095	1.2239	1.3334	7.3473	7.3473	0.0821	−0.0011	1.1180	−0.0005	0.9907
	Summer	WLS	Exponential	0.0001	0.0105	0.0106	6.3270	18.9533	0.0094	0.0003	0.0777	0.0018	0.9974
THI_{Dawn}	Winter	OLS	Spherical	0.0180	0.1811	0.1991	5.6348	5.6348	0.0902	0.0000	0.4376	0.0000	0.9745
	Summer	OLS	Spherical	0.0139	0.1371	0.1510	5.5329	5.5329	0.0924	0.0000	0.3817	0.0000	0.9754
$THI_{Morning}$	Winter	OLS	Spherical	0.0195	0.2087	0.2282	5.6193	5.6193	0.0856	0.0000	0.4720	0.0000	0.9818
	Summer	OLS	Spherical	0.0251	0.2222	0.2473	5.6533	5.6533	0.1014	0.0004	0.4946	0.0004	0.9880
$THI_{Afternoon}$	Winter	WLS	Spherical	0.0195	0.2252	0.2447	6.2174	6.2174	0.0798	0.0000	0.4891	0.0000	0.9882
	Summer	OLS	Spherical	0.0191	0.2116	0.2307	9.8302	9.8302	0.0826	0.0051	0.4223	0.0060	0.9965
THI_{Night}	Winter	OLS	Spherical	0.0185	0.1736	0.1921	5.5382	5.5382	0.0964	0.0000	0.4335	0.0000	0.9821
	Summer	WLS	Spherical	0.0108	0.1170	0.1278	5.8472	5.8472	0.0845	0.0002	0.3560	0.0003	0.9911
$THI_{Minimum}$	Winter	WLS	Spherical	0.0494	0.6455	0.6949	5.7829	5.7829	0.0711	0.0005	0.8241	0.0003	0.9832
	Summer	REML	Spherical	0.0396	0.4477	0.4873	22.3283	22.3283	0.0813	−0.0045	0.4305	−0.0051	0.9991
$THI_{Maximum}$	Winter	OLS	Spherical	0.0494	1.1543	1.2037	5.3953	5.3953	0.0410	0.0002	1.0851	0.0001	0.9815
	Summer	ML	Exponential	0.0838	1.3260	1.4098	12.9800	38.8872	0.0594	0.0097	0.7191	0.0064	0.9737

C_0 - nugget effect; C_1 - contribution; $C_0 + C_1$ - sill; *a* - range; *a′* - practical range; SDI - spatial dependence index; ME - mean-error; SD_{ME} - mean-error standard deviation; SE - standardised-error; SD_{SE} - standardised-error standard deviation; Dawn - mean values during the dawn; Morning - mean values during the morning; Afternoon - mean values during the afternoon; Night - mean values during the night; Maximum - absolute maximum values; Minimum - absolute minimum values; OLS - Ordinary Least Squares; WLS - Weighted Least Squares; ML - Maximum Likelihood; and REML - Restricted Maximum Likelihood. **Units:** C_0, C_1 and C_0+C_1 are expressed in squared units of the corresponding analysed variable ($°C^2$ for T_{db}, $\%^2$ for RH and THI^2 for THI); *a* and *a′* are expressed in metres (m); SDI, ME, SD_{ME}, SE and SD_{SE} are dimensionless statistics.

techniques were used to generate spatial distribution maps for T_{db}, RH, and THI during both winter and summer periods. These maps were used to identify areas exhibiting extreme values for the studied climatic variables (the most thermally challenging conditions), as well as to suggest spatially tailored improvements to the thermal environment, according to the thermal requirements of lactating Holstein dairy cows.

Using geostatistical techniques, it was possible to quantify the magnitude of spatial dependence of T_{db}, RH, and THI inside the CBP system, across different times of day (dawn, morning, afternoon and night), as well as during the extreme conditions, in both winter and summer in Brazil, based on monitoring campaigns conducted over 15 consecutive days in each season. Therefore, the spatial patterns identified reflect intra-seasonal variability under the specific climatic conditions observed during the monitoring periods. Based on cross-validation and the defined selection criteria, the best fits were analysed and chosen for each of the 36 study scenarios used to assess the thermal conditions (Table 3).

For most study scenarios ($n = 32$), the best semivariogram fits were obtained using the Spherical model, while the Exponential and Gaussian models provided the best semivariogram fits for two variables each (Exponential - $RH_{Maximum}$ and $THI_{Maximum}$ in summer; and Gaussian - $T_{db\text{-}Maximum}$ and $RH_{Afternoon}$ in summer; Table 3).

For each scenario, regardless of the model that provided the best fit, the selection was based on metrics calculated through cross-validation. The resulting values were $ME \leq 0.02$ and $SE \leq 0.02$, with SD_{SE} values very close to one ($0.97 \leq SD_{SE} \leq 0.99$). Based on these results, the fitted semivariograms adequately represented the spatial variability of these variables. These findings were consistent with those reported by Ferraz et al. (2019), Andrade et al. (2022), Oliveira et al. (2022), Silva et al. (2023) and Guesine et al. (2023), who also observed that the use of these three models provided the best fits when applying geostatistical techniques to evaluate the spatial dependence of thermal environment variables in animal housing.

One of the most important coefficients in theoretical models for semivariograms is the nugget effect (C_0), which represents the variability that is not explained by the chosen sampling distance (Silva et al., 2021). For all the analysed variables, the values of C_0 were close to zero, indicating that these variables had low unexplained variability and exhibited continuous semivariograms (Table 3). The highest values of C_0 were observed for the situations with absolute minimum RH values during winter and summer, which recorded C_0 values of ~1.50 and ~2.05, respectively. However, in these two situations, high variance was observed in the data sets (~17.74 and ~28.46, respectively). Therefore, considering the sample variance of the data, the C_0 values obtained from the fitted semivariograms for these variables were not deemed high (Table 3).

Despite its importance, C_0 can be attributed to numerous factors, such as errors in data collection and analysis and local or stochastic variations, among other factors. Therefore, it is not possible to quantify the individual impact of each of these factors on its composition (Ferraz et al., 2019). Thus, it is important to use other methodologies for evaluating spatial dependence, such as the SDI (Cambardella et al., 1994). For all the scenarios of the variables and indices analysed, the SDI values were below 0.25 and therefore characterised as indicating strong spatial dependence (Table 3). The highest values were obtained for the variables $RH_{Afternoon}$ in summer and $T_{db\text{-}Morning}$ in summer, with SDI values of ~0.11 and ~0.10, respectively.

Within the scope of the SDI analyses, it is worth noting that the results obtained can be used to assess the suitability of applying geostatistical methods, given the number of sampling points adopted. In general, it is recommended that 100 or more sampling points be used to obtain more robust semivariogram estimates (Webster & Oliver, 1992). However, it is widely recognised and accepted that smaller sample sizes, such as 55 data collection points, are sufficient to detect significant spatial patterns, provided that a strong or moderate spatial correlation is present (He et al., 2022; Kerry & Oliver, 2007). Therefore, considering that strong spatial dependence was observed in all evaluated scenarios, it can be concluded that the use of geostatistical methods is appropriate for this type of case, as the presence of spatial dependence is the essential condition for their application (Ferraz et al., 2014). This is particularly relevant when regular sampling grids are used, as in this study and in other research focused on the environment of intensive animal production facilities, which typically cover significantly smaller areas compared to other fields where geostatistics is applied, such as mining and crop production (Guesine et al., 2023; Silva et al., 2020; Wadoux et al., 2019).

In geostatistics, another relevant parameter is the range (*a*), which represents the distance beyond which spatial dependence between the data is considered negligible (Ferraz et al., 2019). In this study, the evaluated variables exhibited varying values for *a* (Table 3), but all of them were consistently greater than the minimum sampling distance (4.50 m), thus supporting the hypothesis of spatial dependence (Oliveira et al., 2024). The highest values for *a* were observed for the variables $T_{db\text{-}Maximum}$ in winter (recorded in the afternoon) and $T_{db\text{-}Afternoon}$ in summer (~41.72 m and ~31.06 m, respectively). These results suggested that T_{db} exhibited greater spatial dependence in the afternoon, which could be related to insufficient air renewal within the studied CBP system during this period (Silva et al., 2021). This may indicate that the mechanical ventilation system in place was inadequate to ensure uniform environmental conditions. On the other hand, the lowest values of *a* were recorded for RH_{Night} and $T_{db\text{-}Night}$ in winter (~5.33 m and ~5.29 m, respectively), indicating that these variables exhibited less spatial dependence at that time. The lowest values of *a* obtained can be used to determine the distance between sampling points in future studies. Specifically, it can be inferred that distances of up to 5.29 m may be considered adequate for evaluating the spatial dependence of T_{db}, RH, and THI.

In addition to supporting the assumption of spatial dependence, *a* is the maximum distance at which observations remain spatially correlated within the AOZ. However, from a biological and environmental standpoint, it can be interpreted as the characteristic dimension of zones with relatively homogeneous microclimatic conditions inside the facility. In CBP systems, where animals are free to move and tend to concentrate in areas with more favourable thermal conditions, this spatial scale becomes particularly relevant, as it reflects the extent to which environmental heterogeneity may influence animal distribution and behaviour. Studies conducted in similar housing systems have shown that spatial variability in thermal conditions directly affects animal positioning, occupancy patterns, and consequently welfare and productivity (Andrade et al., 2022; Oliveira et al., 2022; Silva et al., 2020).

Therefore, the *a* values observed in the present study, which varied from ~5.00 m to over 40.00 m depending on the variable and period of the day, indicated that the thermal environment within the CBP system was structured at multiple spatial scales. Shorter ranges suggested the presence of localised gradients, possibly associated with micro-scale factors, such as airflow obstruction, moisture distribution in the bedding, or animal clustering, whereas larger ranges indicated broader zones of spatial continuity, typically associated with the overall configuration of the ventilation system and building geometry (Ferraz et al., 2019; Silva et al., 2021). This multiscale spatial structure reinforces the need to interpret thermal conditions as spatially organised patterns resulting from the interaction between structural design, environmental control systems, and animal activity and not as being uniform across the facility.

From a practical perspective, the *a* values observed in this study have direct implications for the design and management of environmental control strategies. When the spatial dependence occurs at relatively short distances, as observed in several scenarios, localised interventions tend to be more effective than uniform adjustments across the entire facility. In such cases, strategies, such as the repositioning or redistribution of fans, adjustments in airflow direction, and targeted use of evaporative cooling systems, may contribute more efficiently to improving thermal conditions within specific zones of the AOZ. This approach is consistent with previous studies that highlight the importance of spatially explicit management in CBP systems, demonstrating that geostatistical analysis can be used as a decision-support tool for optimising environmental control strategies in livestock housing systems (Andrade et al., 2022; Guesine et al., 2023; Oliveira et al., 2022). Therefore, the interpretation of *a* extends beyond its statistical role, providing a quantitative basis for linking spatial dependence to biological responses and guiding more efficient and targeted thermal management strategies.

The results from geostatistical modelling revealed that the environmental variables did not exhibit random distribution, as evidenced by the strong spatial dependence and *a* values consistently greater than the minimum distance between sampling points (Silva et al., 2021). In this context, the identified spatial structures provided the basis for applying ordinary kriging to estimate values of the thermal environmental variables at unsampled locations within the CBP system and to generate spatial distribution maps for T_{db}, RH and THI (Figs. 6–11). These maps make it possible to assess the spatial behaviour of the variables of interest and to identify zones with unfavourable thermal conditions, thereby supporting the implementation of targeted environmental management strategies (Curi et al., 2017).

The CV values obtained for the average datasets of T_{db}, RH and THI used to create the spatial distribution maps were always below 0.10 (Figs. 6–11). This indicated that the data recorded during both periods (winter and summer) exhibited low dispersion, according to the classification suggested by Gomes (2000). These results suggested that there was relative homogeneity for all the mapped variables within the CBP system (Franco et al., 2022).

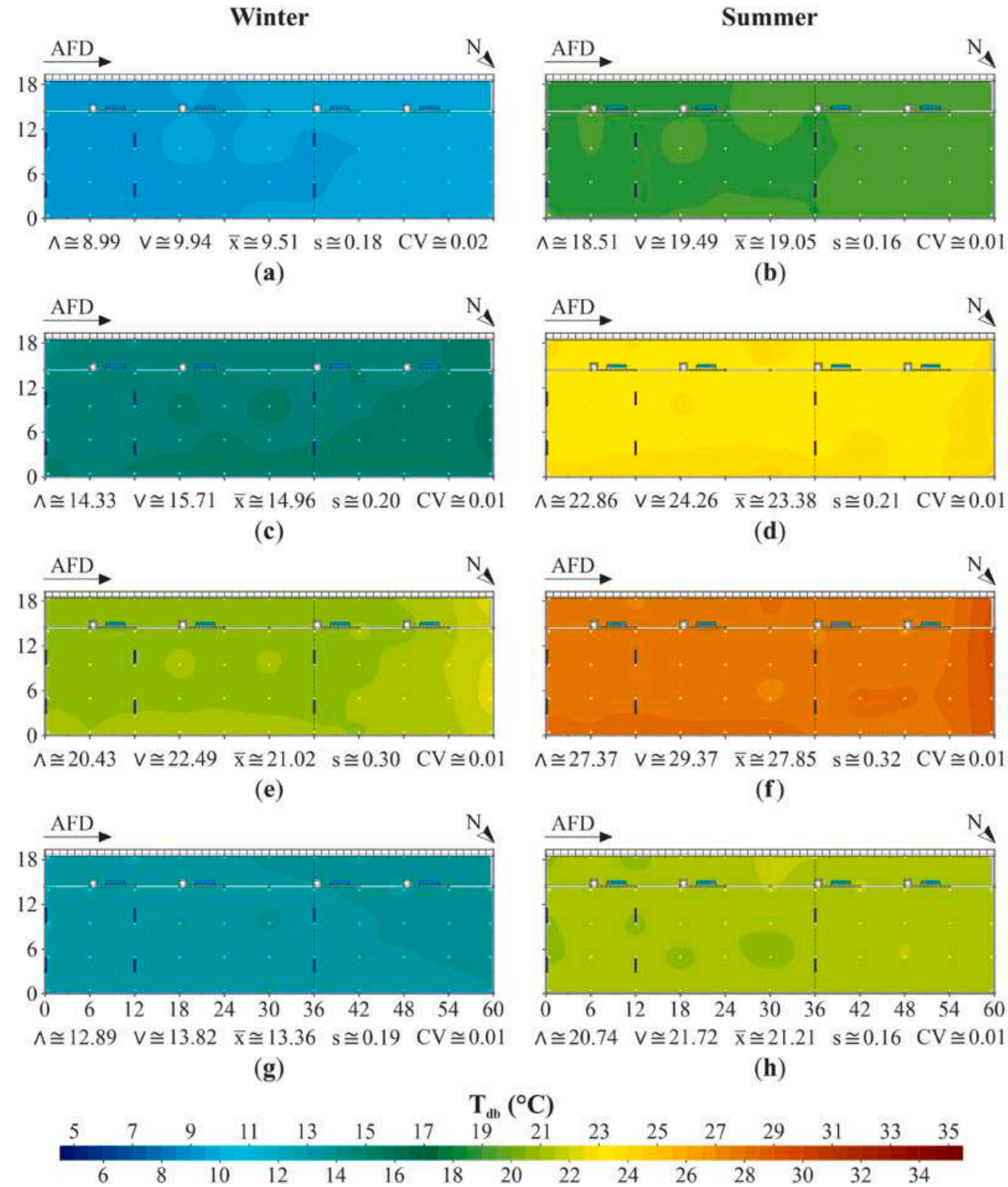

Fig. 6. Spatial distribution of dry-bulb air temperature values (T_{db}, in °C) inside the Compost-Bedded Pack Barn system under study: mean values for periods **(a)** dawn, **(c)** morning, **(e)** afternoon and **(g)** night in winter; and mean values for periods **(b)** dawn, **(d)** morning, **(f)** afternoon and **(h)** night in summer. ∧ - minimum; ∨ - maximum; $\bar{x}$ - mean; s - standard deviation; CV - coefficient of variation; AFD - airflow direction; N - North indication; axes values are in metres (m).

In both winter and summer, low spatial variability in the average T_{db} values was observed during the early morning and night, with the variation amplitudes (ΔT_{db}) across the CBP system being $< 1.00\,°C$ (Fig. 6a, b, 6g, and 6h). In contrast, during the morning and afternoon periods, higher average ΔT_{db} was observed, particularly in the afternoon, when ΔT_{db} was 2.06 °C in winter and 2.00 °C in summer (Fig. 6e and f). Despite similar variation amplitudes for $T_{db\text{-}Afternoon}$ during winter and summer, the thermal conditions were more challenging in summer, when the average T_{db} ranged between 27.37 and 29.37 °C, significantly exceeding the UTCL for lactating dairy cattle (24.00 °C). The high T_{db} values recorded during the summer may have negatively impacted the welfare and productive performance of the lactating Holstein cows housed in the CBP system (Herbut et al., 2018; Morales-Piñeyrúa et al., 2022).

In both monitored periods (winter and summer), a small gradient of T_{db} was observed throughout the CBP system during the morning and afternoon, with higher values consistently recorded in the northwest region of the CBP system (Fig. 6c–f). The high T_{db} values recorded in this region of the CBP system, particularly in the afternoon, further indicated insufficient air renewal in this area of the system, as evidenced by the greater spatial dependence (higher a).

According to Damasceno (2020), in CBP systems with positive-pressure mechanical ventilation using low-volume and high-speed fans, like the CBP system used here, it is recommended that the maximum distance between ventilation lines be 12.00 m to maintain uniform air renewal rates across the AOZ. In this study, it was found that this distance was only met in the Southeast region of the CBP system, between ventilation lines 1 and 2 (Fig. 1). Throughout the remaining longitudinal length of the CBP system, there was only one ventilation line (line 3), which was located 24.00 m away from other lines and the Northwest end. Thus, the results observed in the Northwest region of the CBP system suggested that the third ventilation line was inadequate for ensuring homogeneous temperature conditions in its operational area (Fig. 6c–f), despite being continuously operational (24 h day^{-1}).

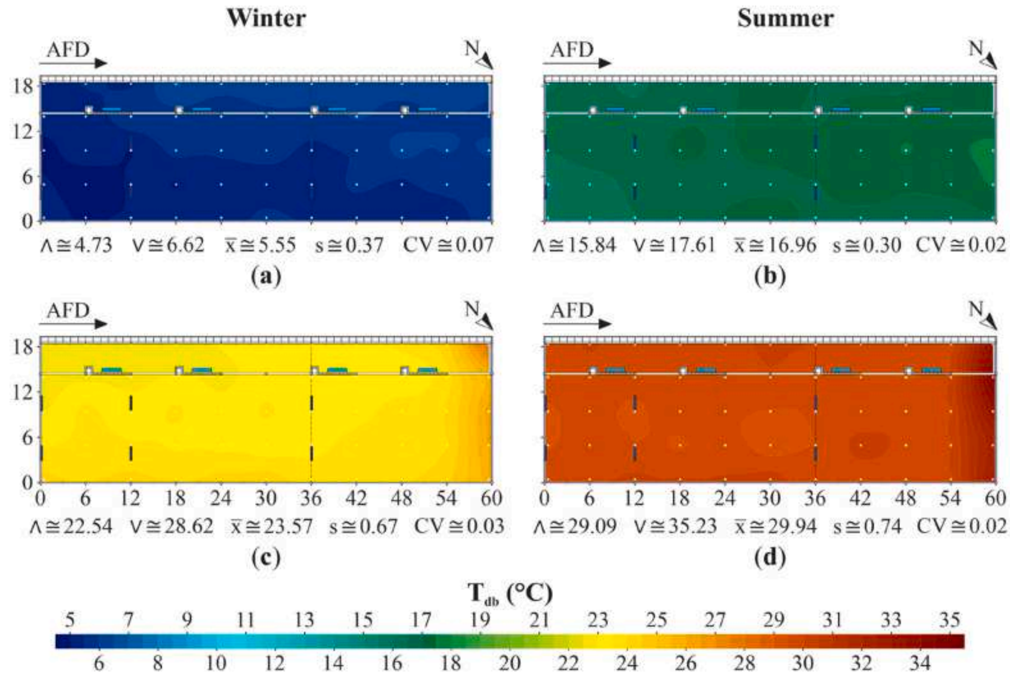

Fig. 7. Spatial distribution of dry-bulb air temperature values (T_{db}, in °C) inside the Compost-Bedded Pack Barn under study: **(a)** absolute minimum values and **(c)** absolute maximum values in winter; and **(b)** absolute minimum values and **(d)** absolute maximum values in summer. Symbols as for Fig. 6. Axes values are in metres (m).

Regarding the formation of the T_{db} gradient across the CBP system area during daylight hours (morning and afternoon), the most problematic scenario for each monitoring period occurred in the afternoon. During this time, the highest average values were recorded in the Northwest region of the CBP system ($T_{db} \geq 21.50$ °C in winter; and $T_{db} \geq 28.00$ °C in summer; Fig. 6e and f). In the afternoon period, it was observed that direct solar radiation affected this region. Consequently, the higher T_{db} values recorded in the last 6.00 m of the CBP system were due to the heating of the air from shortwave radiation (Andrade et al., 2022; Tao et al., 2020). In the Northwest region of the CBP system, the incidence of direct solar radiation was due to two factors: the incorrect orientation of the facility's longitudinal axis and the lack of frontal closures on the gable ends.

Although the spatial pattern of average T_{db} by period was mapped (Fig. 6), it was also deemed important to assess the spatial distribution at times when absolute minimum and maximum values of this variable were recorded, as these conditions are considered extreme for animal thermoregulation (Fig. 7). High T_{db} peaks are particularly challenging for thermal comfort and when sustained for extended periods, they can lead to significant productive and reproductive losses, impair health, or even result in death in the most extreme cases (Cartwright et al., 2022; Gernand et al., 2019).

In both monitoring periods, the recorded absolute minimum values of T_{db} were above 5.00 °C, falling below this threshold only in a small area located between ventilation lines 1 and 2 and only in winter (Fig. 7a). Therefore, the was no significant thermal stress due to cold, as most animals can tolerate this temperature level with relative ease (De Masi et al., 2021).

However, the maps of absolute maximum values of T_{db} [winter: day 14 at 1:45 p.m. (Fig. 4a); and summer: day 6 at 2:50 p.m (Fig. 4a).] showed that temperatures exceeded 24.00 °C, even during the cold season (Fig. 7c and d). In the winter period, values above the UTCL were observed only in the area near the northwest face of the CBP system, within the last 6 m (Fig. 7c). In contrast, during the summer, the prevalence of T_{db} values $\geq$ 29.00 °C was observed throughout the entire AOZ, with the highest values also recorded in the Northwest region, with $T_{db} \geq 30.00$ °C (Fig. 7d). Given that the T_{db} curve during this period exhibited a well-defined pattern (Fig. 4a), it was understood that the occurrence of T_{db} values $\geq$ 29.00 °C was consistent across all monitored days and was not limited to the Northwest region of the CBP system, as was implied by Fig. 6f.

In addition to T_{db}, it is crucial to assess the spatial distribution of RH (Figs. 8 and 9). For the average RH values by time of day, very similar spatial patterns were observed in both winter and summer, with values predominantly > 87.00% during the dawn and night periods (Fig. 8a, b, 8g, and 8h). During the morning and afternoon periods (Fig. 8c, d, 8e, and 8f), RH levels were decreasing, with less homogeneous spatial distribution within the system. The lowest average values were recorded in the peripheral areas of the CBP system, which are more influenced by external conditions (Oliveira et al., 2022). These RH results aligned with those reported by Andrade et al. (2022), who mapped thermal conditions in a closed CBP system located in the same region as this study.

During the dawn, morning, and night periods (Fig. 8a, b, 8g, and 8h), the average RH levels remained above the recommended range for housing dairy cattle, which is 30.00-80.00% according to Nääs (1989). Although these conditions occurred during times when the average T_{db} levels were considered thermally comfortable (Fig. 6a, b, 6g, and 6h), it is important to highlight that the prevalence of high RH levels in such a system can lead to excessive bedding moisture, increase animal soiling, compromise milk quality, and cause health issues in the animals (Blanco-Penedo et al., 2020; Eckelkamp et al., 2016; Leso et al., 2020). Therefore, high RH values are undesirable and further indicated that the mechanical ventilation systems at the location were either inadequately sized and/or managed, and therefore insufficient for effectively reducing RH levels.

The average RH values throughout the internal area of the CBP system studied remained below 70.00% during the times with the highest average T_{db} values (Figs. 5, 6, and 8) and were even lower during the periods with the highest absolute T_{db} values (Figs. 7 and 9). These results suggested that there is potential for leveraging evaporative cooling of the air through the use of evaporative padding cooling panels combined with negative pressure mechanical ventilation, or even misting combined with positive pressure ventilation (limited to the feeding alley), in this type of confinement system during the hotter times

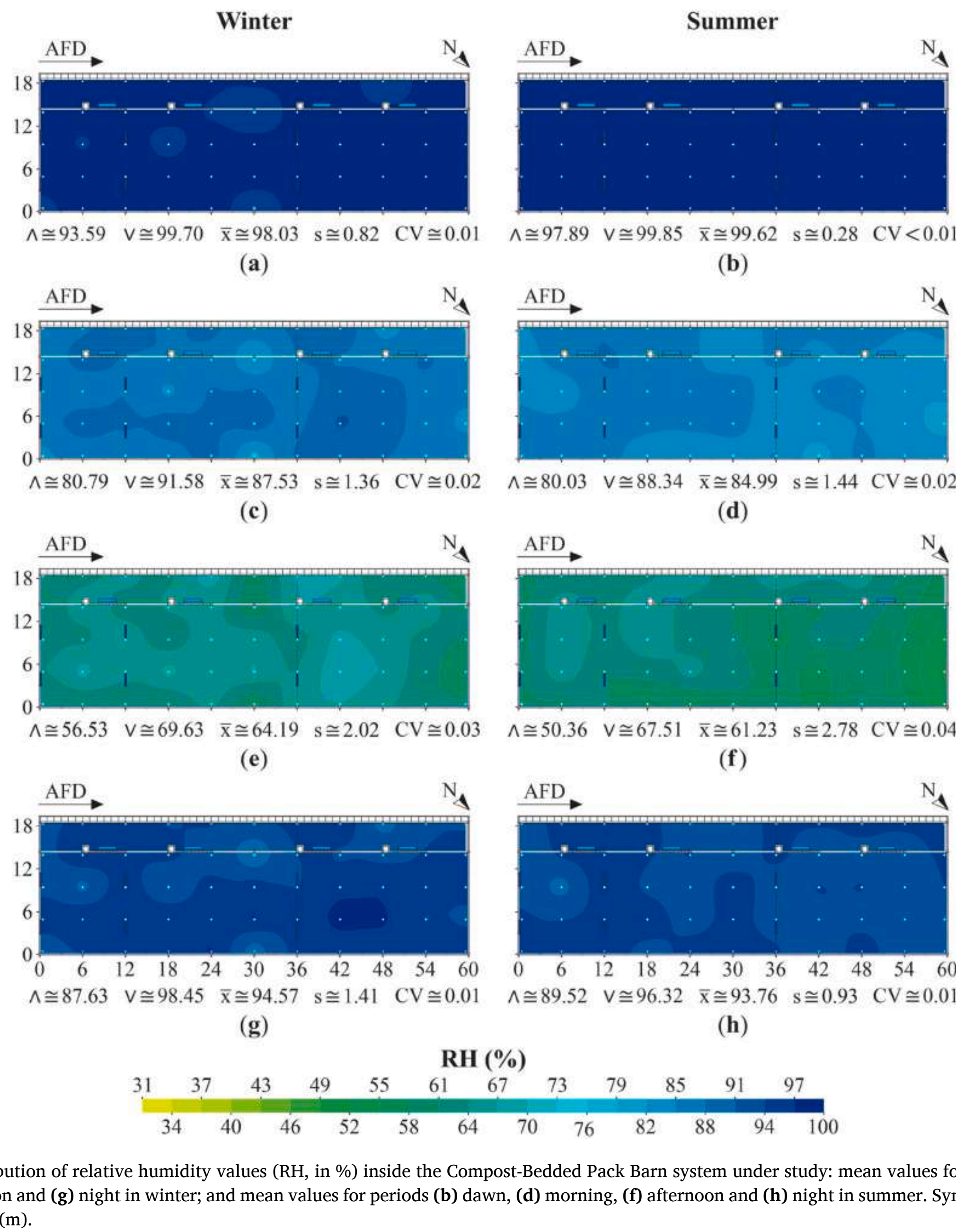

Fig. 8. Spatial distribution of relative humidity values (RH, in %) inside the Compost-Bedded Pack Barn system under study: mean values for periods **(a)** dawn, **(c)** morning, **(e)** afternoon and **(g)** night in winter; and mean values for periods **(b)** dawn, **(d)** morning, **(f)** afternoon and **(h)** night in summer. Symbols as for Fig. 6. Axes values are in metres (m).

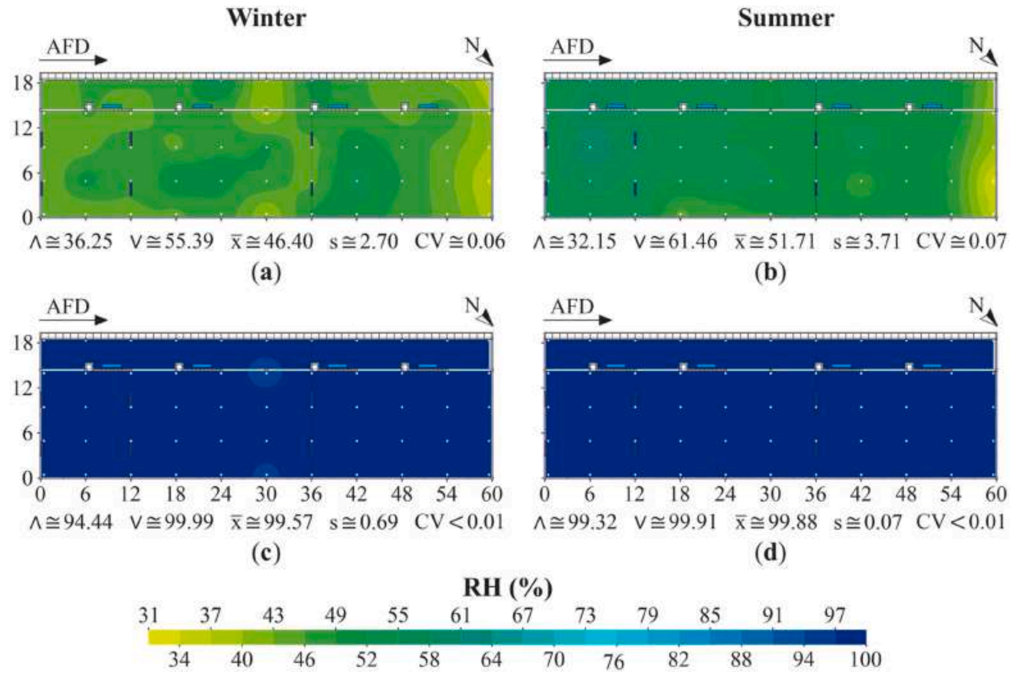

Fig. 9. Spatial distribution of relative humidity values (RH, in %) inside the Compost-Bedded Pack Barn under study: **(a)** absolute minimum values and **(c)** absolute maximum values in winter; and **(b)** absolute minimum values and **(d)** absolute maximum values in summer. Symbols as for Fig. 6. Axes values are in metres (m).

of the day and year. However, it is important to emphasise that such methods should only be employed during hot and dry periods. In hot and dry periods, as depicted for summer afternoons in this study (Figs. 6–9), it can be inferred that the use of the thermal defence systems could effectively reduce T_{db} values, provided these systems are properly designed and managed (Arcidiacono, 2018; Mrema et al., 2011).

At the times when minimum and maximum absolute RH values were recorded, similar patterns were observed in both winter and summer (Fig. 9). Through the analysis of maximum absolute values, it was found that there was low spatial variability, with RH levels always exceeding 94.00% (Fig. 9c and d). This condition was observed during the night in both winter and summer on all monitored days (Fig. 4b), due to thermal inversion.

The spatial distribution maps of the minimum absolute RH values revealed high spatial variability (ΔRH >15.00%), with the lowest values consistently recorded in the Northwestern region of the CBP system, attributed to the effect of direct solar radiation (Fig. 9a and b). Although these results indicated that the ventilation system was ineffective in ensuring uniform RH conditions, the values observed fell within the recommended range for housing dairy cattle (30.00-80.00%).

Since it was of interest in this study to assess the combined effect of T_{db} and RH on the spatial behaviour of average thermal conditions at different times of the day, both during winter and summer, spatial distribution maps of THI were also generated (Fig. 10). For the average THI values by time of day, low spatial variability was observed, with the greatest average amplitudes occurring during the morning and afternoon periods (ΔTHI > 2.00). The maps revealed that the average thermal conditions remained approximately homogeneous across the AOZ, except for the Northwest region of the CBP system, where THI was higher during the morning and afternoon (Fig. 10c, d, 10e and 10f).

When analysing the thermal environment based on the THI ranges cited by Hahn (1999), it was observed that during winter, the average conditions were maintained at levels considered normal (Fig. 10a, c, 10e, and 10g), even falling below 72.00, a value deemed by many authors as the UTCL for high-producing dairy cows (Bleizgys et al., 2022; Herbut et al., 2018).

For the absolute maximum THI values recorded during winter (Fig. 11c), levels exceeding 74.00 were only observed in a small area at the north-western end of the CBP system under study, specifically in the feeding alley. Therefore, these values were of limited representativeness. Based on these results, throughout the winter, thermally comfortable conditions for the animals were maintained throughout the entire AOZ.

In contrast, it was observed that the average THI during summer afternoons remained above 74.00 (normal) throughout the entire AOZ of the studied CBP system (Fig. 10f). These conditions were even more challenging during times with absolute maximum values (Fig. 11c and d), where, in the worst case, THI values exceeded 77.00 across the entire AOZ (alert to danger conditions; Fig. 11d).

The average results for THI reported in this study, during the morning and afternoon periods (Fig. 10c, d, 10e, and 10f), corroborate with those obtained by Mota et al. (2019), who analysed thermal conditions in an open-sided CBP system with low-volume and high-rotation fans in the South of Minas Gerais, during winter and summer periods. With the ventilation system in operation (the same condition as in this study), Mota et al. (2019) observed that average THI values were < 74.00 during the mornings and afternoons in winter. However, the thermal conditions during summer afternoons were considered thermally stressful in some areas of the CBP system (THI ≥ 74.00), although they were characterised as normal thermal comfort conditions during the morning.

The average THI results also aligned with those reported by Andrade et al. (2022) for a closed CBP system, which used evaporative cooling pads combined with negative pressure mechanical ventilation and was in the same study region (Zona da Mata, Minas Gerais, Brazil). Andrade et al. (2022) mapped the thermal conditions and found that the average THI values were always < 74.00 during winter. However, they observed average values exceeding this threshold across the entire area of the CBP system during summer afternoons.

Since the housed animals were high-producing dairy cows (30.00-35.00 kg animal^{-1} day^{-1}), it can be inferred that the elevated THI values observed during summer afternoons (Fig. 10f and 11d) may have negatively affected their dry matter intake (Collier et al., 2019), as well as their lying time, which could be reduced by up to 3.30 h day^{-1} (Nordlund et al., 2019). The reduction in average daily milk production per animal observed during the summer period (Table 1) may be due to

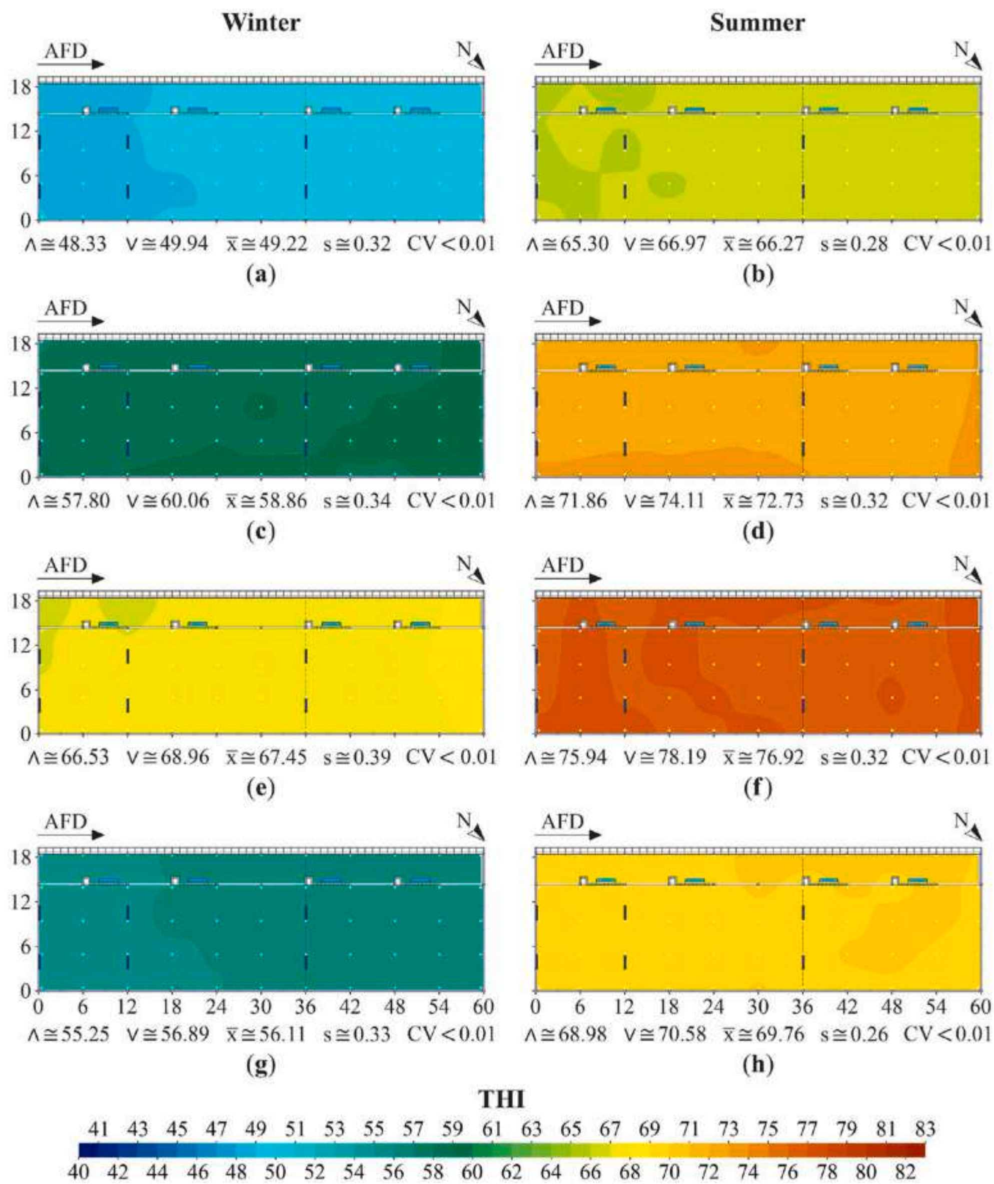

Fig. 10. Spatial distribution of Temperature and Humidity Index (THI) inside the Compost-Bedded Pack Barn system under study: mean values for periods **(a)** dawn, **(c)** morning, **(e)** afternoon and **(g)** night in winter; and mean values for periods **(b)** dawn, **(d)** morning, **(f)** afternoon and **(h)** night in summer. Symbols as for Fig. 6. Axes values are in metres (m).

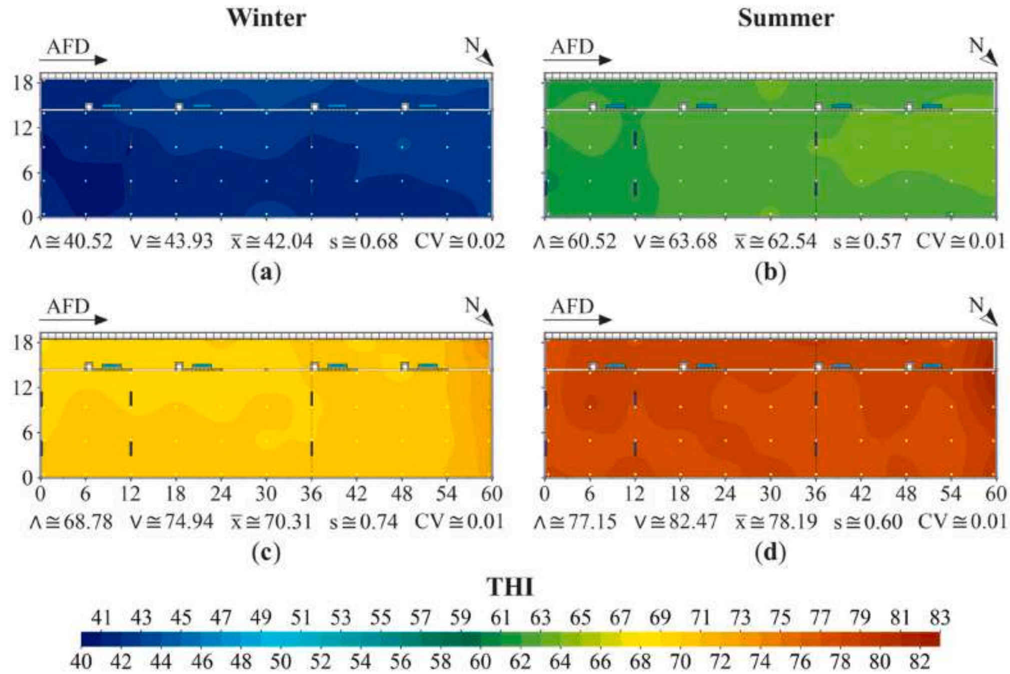

Fig. 11. Spatial distribution of Temperature and Humidity Index (THI) inside the Compost-Bedded Pack Barn under study: **(a)** absolute minimum values and **(c)** absolute maximum values in winter; and **(b)** absolute minimum values and **(d)** absolute maximum values in summer. Symbols as for Fig. 6. Axes values are in metres (m).

physiological and behavioural responses to heat stress, as outlined by Gunn et al. (2019) and Tao et al. (2020). For high-producing dairy cows (>30.00 kg day^{-1}), this reduction may be attributed to multiple factors, including decreased dry matter and water intake, as well as reduced milk synthesis, as the animals attempt to lower their heat production (Collier et al., 2019).

In addition to affecting dry matter intake, resting time and milk production, it is important to note that thermal stress conditions, such as those observed in this study during summer afternoons (Fig. 10f and 11d), can also trigger health and reproductive issues in the animals. According to Tao et al. (2020), typical summer environmental conditions are often associated with an increase in clinical mastitis incidence and somatic cell count. This is attributed to the greater growth of environmental pathogens, combined with the negative impact of thermal stress on immune function. As animals tend to stand for longer periods under heat stress conditions, there is often an increase in the incidence of hoof problems (such as lesions, white line disease, interdigital hyperplasia, etc.) and lameness (Biasato et al., 2019; Polsky & von Keyserlingk, 2017; Reuscher et al., 2023). In addition, heat stress can negatively impact reproductive indices (Rodríguez-Godina et al., 2024; Sammad et al., 2020; Tao et al., 2020), a condition that is often only observed several months later.

3.4. *Recommendations for improving the thermal environment in the compost-bedded pack barn (CBP) systems*

Based on the results obtained from the temporal and spatial analyses (Figs. 4–11), practical recommendations are proposed to improve thermal conditions in the evaluated CBP system under contrasting seasonal scenarios. These recommendations may also support the retrofit of existing facilities and the design of new CBP projects, provided that local climatic and geographical conditions are considered.

In situations like the CBP system, where the longitudinal axis was oriented Northwest-Southeast (Fig. 1), it is recommended to construct closure structures (wood, metal, fiber cement, etc.), either fixed or movable, at the upper part of the gable. The aim is to reduce the direct entry of solar radiation and, consequently, reduce average values of T_{db} and THI (Herbut et al., 2018; Oliveira et al., 2022). Alternatively, and complementarily, planting deciduous trees (which shed their leaves at the beginning of winter) near the Northwest side of the CBP system could be considered. Provided that the lower trunks are pruned, these trees will not obstruct natural ventilation but will shade the area that receives direct solar radiation during the hottest periods. This strategy may reduce solar heat gain and improve thermal conditions within the AOZ (De Masi et al., 2021; Pons et al., 2023). It is important to note that the implementation of the latter solution (planting vegetation strips) requires a thorough preliminary study to address aspects such as the type and size of trees to be used for the region's climate and soil, and the distance of the vegetation strips from the facility, among other factors.

Values of $T_{db} \geq 29.00\,^{\circ}C$ were recorded on all monitored days during the summer, and this condition was not limited to the Northwest region of the CBP system (Fig. 5a and 7d). These strategies alone would not be sufficient to ensure thermal comfort for dairy cows during summer. Additional cooling strategies would be required to further improve the thermal environment within the CBP system.

Based on the results depicted for average data (Fig. 6f and 10f) and maximum absolute values of T_{db} and THI (Fig. 7d and 11f), it was observed that values above 24.00 °C and 74.00, respectively, were prevalent throughout the entire AOZ during summer afternoons. These results provide evidence that simply increasing the ventilation rate in this CBP system would be insufficient to ensure comfortable thermal conditions for the Holstein dairy cows housed in the system during this period. Therefore, it was concluded that the use of animal body cooling methods (such as water sprinkling) and/or evaporative air cooling (such as water misting), when combined with well-designed and managed mechanical ventilation systems, would be the most suitable strategy for hotter periods in CBP systems similar to the one evaluated.

In this study, animal body cooling via a parallel water sprinkling line positioned next to the cows' feeding troughs was carried out whenever the T_{db} exceeded 24.00 °C. However, the results showed that the T_{db} values in the feeding alley were only minimally affected by the evaporation of water droplets falling onto the floor when this system was in operation in summer during the late morning and throughout the afternoon (Fig. 6e, f, and 7d). This happened because the fans in the facility were only distributed in the bedding area of the CBP under study, which, due to the presence of guardrails around the water troughs, typically resulted in the formation of areas with low airspeed in the feeding alley (Oliveira et al., 2023). The absence of fans in the feeding alley limited the potential for cooling both the animals and the environment through water spraying, as ventilation is essential for promoting air movement over the animals' bodies and the floor, and for enhancing the evaporation of the sprayed water droplets (Arcidiacono, 2018; Fournel et al., 2017; Polsky & von Keyserlingk, 2017). Cooling the animals in the feeding alley may not be sufficient to mitigate the adverse effects of heat stress during extremely hot periods. Therefore, it would be necessary to either redesign this body cooling system or combine it with air cooling methods during the hottest periods of the day throughout the year.

A third alternative to improve the thermal environment during hot periods in this CBP system would be to enclose the CBP and use wetted cellulose pads in combination with a negative-pressure mechanical ventilation systems. This setup channels and moves the entire air volume with greater uniformity and pressure through the action of exhaust fans. This air-cooling method forces hot air through a wetted porous material pad. As the air passes through the wetted pad, simultaneous heat and mass exchange occurs and sensible heat is converted into latent heat and used for the phase change of water (reducing T_{db}); and some of the water in the air is converted into vapor (increasing RH) (Andrade et al., 2024; Fournel et al., 2017; Mrema et al., 2011). However, it is important to note that the use of evaporative cooling systems for reducing T_{db}, whether through misting or wetted pads, is primarily recommended for hot and dry periods (when RH is lower), as a gradient in vapor pressure between the air entering and exiting the wetted pad is necessary (Arcidiacono, 2018). In addition, when using evaporative cooling methods in CBP systems, it is essential to increase the available bedding area per animal, as there is a tendency for increased moisture in the compost bedding (Andrade et al., 2024).

4. Conclusions

This study demonstrated that the validated low-cost embedded system enabled the continuous characterisation of the temporal and spatial behaviour of the microenvironment within an open Compost-Bedded Pack Barn. The results confirmed the initial hypothesis by showing that the thermal environment in naturally ventilated CBP facilities is dynamic and spatially heterogeneous, varying with both season and time of day. The monitored microenvironment generally remained within the thermal comfort zone for lactating Holstein cows during winter, whereas summer measurements revealed prolonged periods of heat stress, while also identifying periods favourable for the strategic use of evaporative cooling.

These findings demonstrate that environmental control strategies in open CBP systems should account for both temporal dynamics and spatial heterogeneity rather than being uniformly applied throughout the facility. The proposed monitoring approach provides a practical and economically viable tool for precision environmental management and establishes a scientific basis for the design, retrofitting, and operation of naturally ventilated dairy housing systems under different climatic scenarios.

Funding

This work was supported by the National Council for Scientific and Technological Development, Brazil [CNPq; Grant Numbers 151546/2024-0 and 200081/2025-0]; Coordination of Superior Level Staff Improvement, Brazil [CAPES; Finance Code 001]; and Research Supporting Foundation of Minas Gerais State, Brazil [FAPEMIG; Finance Code 001].

CRediT authorship contribution statement

Carlos Eduardo Alves Oliveira: Conceptualization, Data curation, Investigation, Methodology, Software, Validation, Visualization, Writing – original draft, Writing – review & editing. **Ilda de Fátima Ferreira Tinôco:** Conceptualization, Data curation, Funding acquisition, Methodology, Project administration, Resources, Supervision, Validation, Writing – review & editing. **Túlio Souza Mariano:** Data curation, Investigation. **Fernanda Campos de Sousa:** Methodology, Supervision, Writing – review & editing. **Rafaella Resende Andrade:** Conceptualization, Data curation, Funding acquisition, Methodology, Project administration, Resources, Supervision, Validation, Writing – review & editing. **Flávio Alves Damasceno:** Conceptualization, Methodology, Supervision, Writing – review & editing. **Gabriel Araújo e Silva Ferraz:** Methodology, Supervision, Writing – review & editing. **Matteo Barbari:** Conceptualization, Methodology, Supervision, Writing – review & editing.

Declaration of competing interest

The authors declare that they have no known competing financial interests or personal relationships that could have appeared to influence the work reported in this paper.

Acknowledgments

The authors would like to thank the following for their financial support of this project: the CNPq, Brazil; the CAPES, Brazil; and the FAPEMIG, Brazil.

Appendix C. Supplementary data

Supplementary data to this article can be found online at https://doi.org/10.1016/j.biosystemseng.2026.104556.

Appendix A

Table A1
Calibration curves obtained for the DHT22 sensors that comprised the embedded system used for monitoring the thermal environment in the Compost-Bedded Pack Barn system under study (indoor environment) and in the meteorological shelter (outdoor environment).

Sensor	Dry-bulb air temperature (T_{db}, °C)		Relative humidity (RH, %)	
	Equation	R^2	Equation	R^2
1	$T_{db\text{-}Adj} = 0.7537 \times T_{db\text{-}R} + 2.5482$	0.9746	$RH_{Adj} = 0.9094 \times RH_R + 2.4945$	0.9685
2	$T_{db\text{-}Adj} = 0.7652 \times T_{db\text{-}R} + 2.5025$	0.9727	$RH_{Adj} = 0.9456 \times RH_R - 2.4435$	0.9771
3	$T_{db\text{-}Adj} = 0.7938 \times T_{db\text{-}R} + 1.8508$	0.9778	$RH_{Adj} = 0.9262 \times RH_R - 2.4946$	0.9787
4	$T_{db\text{-}Adj} = 0.7836 \times T_{db\text{-}R} + 1.7469$	0.9765	$RH_{Adj} = 0.9204 \times RH_R + 1.6783$	0.9787
5	$T_{db\text{-}Adj} = 0.8216 \times T_{db\text{-}R} + 1.6044$	0.9804	$RH_{Adj} = 0.8582 \times RH_R + 1.5946$	0.9695
6	$T_{db\text{-}Adj} = 0.9013 \times T_{db\text{-}R} + 0.7191$	0.9816	$RH_{Adj} = 1.0081 \times RH_R - 6.8639$	0.9790
7	$T_{db\text{-}Adj} = 0.9153 \times T_{db\text{-}R} + 0.5547$	0.9802	$RH_{Adj} = 1.1801 \times RH_R - 24.408$	0.9733
8	$T_{db\text{-}Adj} = 0.9068 \times T_{db\text{-}R} + 0.3220$	0.9816	$RH_{Adj} = 1.1809 \times RH_R - 22.444$	0.9288
9	$T_{db\text{-}Adj} = 0.9067 \times T_{db\text{-}R} + 0.3482$	0.9889	$RH_{Adj} = 1.0204 \times RH_R - 9.0888$	0.9761
10	$T_{db\text{-}Adj} = 0.8539 \times T_{db\text{-}R} +1.5322$	0.9804	$RH_{Adj} = 1.0168 \times RH_R + 8.9198$	0.9855
11	$T_{db\text{-}Adj} = 0.9189 \times T_{db\text{-}R} + 0.5240$	0.9810	$RH_{Adj} = 1.1351 \times RH_R - 16.352$	0.9917
12	$T_{db\text{-}Adj} = 0.9284 \times T_{db\text{-}R} + 0.6750$	0.9805	$RH_{Adj} = 1.0948 \times RH_R - 16.639$	0.9798
13	$T_{db\text{-}Adj} = 0.9253 \times T_{db\text{-}R} + 0.0879$	0.9789	$RH_{Adj} = 1.0211 \times RH_R - 12.561$	0.9823
14	$T_{db\text{-}Adj} = 0.9005 \times T_{db\text{-}R} + 0.6915$	0.9872	$RH_{Adj} = 0.9802 \times RH_R - 9.4452$	0.9816
15	$T_{db\text{-}Adj} = 0.8694 \times T_{db\text{-}R} + 1.3275$	0.9799	$RH_{Adj} = 1.0134 \times RH_R - 11.409$	0.9856
16	$T_{db\text{-}Adj} = 0.9277 \times T_{db\text{-}R} + 0.7873$	0.9830	$RH_{Adj} = 1.1184 \times RH_R - 20.527$	0.9815
17	$T_{db\text{-}Adj} = 0.9279 \times T_{db\text{-}R} + 0.2991$	0.9804	$RH_{Adj} = 1.2398 \times RH_R - 30.023$	0.9852
18	$T_{db\text{-}Adj} = 0.9285 \times T_{db\text{-}R} + 0.4795$	0.9791	$RH_{Adj} = 1.1164 \times RH_R - 18.294$	0.9888
19	$T_{db\text{-}Adj} = 0.8995 \times T_{db\text{-}R} + 0.5891$	0.9857	$RH_{Adj} = 1.0216 \times RH_R - 11.148$	0.9905
20	$T_{db\text{-}Adj} = 0.8611 \times T_{db\text{-}R} + 1.4975$	0.9737	$RH_{Adj} = 1.2139 \times RH_R - 27.851$	0.9887
21	$T_{db\text{-}Adj} = 0.9464 \times T_{db\text{-}R} + 0.4159$	0.9779	$RH_{Adj} = 1.2080 \times RH_R - 27.993$	0.9791
22	$T_{db\text{-}Adj} = 0.9447 \times T_{db\text{-}R} + 0.4105$	0.9782	$RH_{Adj} = 1.2727 \times RH_R - 32.147$	0.9825
23	$T_{db\text{-}Adj} = 0.9316 \times T_{db\text{-}R} + 0.6428$	0.9780	$RH_{Adj} = 1.0272 \times RH_R - 7.0332$	0.9899
24	$T_{db\text{-}Adj} = 0.8901 \times T_{db\text{-}R} + 1.2578$	0.9808	$RH_{Adj} = 1.0548 \times RH_R - 12.509$	0.9854
25	$T_{db\text{-}Adj} = 0.8751 \times T_{db\text{-}R} + 1.4145$	0.9826	$RH_{Adj} = 1.1630 \times RH_R - 24.294$	0.9813
26	$T_{db\text{-}Adj} = 0.9601 \times T_{db\text{-}R} - 0.0063$	0.9745	$RH_{Adj} = 1.0260 \times RH_R - 6.9375$	0.9857
27	$T_{db\text{-}Adj} = 0.9405 \times T_{db\text{-}R} + 0.7319$	0.9793	$RH_{Adj} = 1.0696 \times RH_R - 15.738$	0.9830
28	$T_{db\text{-}Adj} = 0.9240 \times T_{db\text{-}R} + 0.3840$	0.9791	$RH_{Adj} = 1.1473 \times RH_R - 22.956$	0.9819
29	$T_{db\text{-}Adj} = 0.9058 \times T_{db\text{-}R} + 1.0860$	0.9854	$RH_{Adj} = 1.0427 \times RH_R - 15.139$	0.9834
30	$T_{db\text{-}Adj} = 0.8669 \times T_{db\text{-}R} - 1.5592$	0.9832	$RH_{Adj} = 1.1377 \times RH_R - 11.453$	0.9773
31	$T_{db\text{-}Adj} = 0.9770 \times T_{db\text{-}R} - 0.0086$	0.9722	$RH_{Adj} = 1.2049 \times RH_R - 25.813$	0.9755
32	$T_{db\text{-}Adj} = 0.9466 \times T_{db\text{-}R} + 0.5894$	0.9796	$RH_{Adj} = 0.9710 \times RH_R - 11.285$	0.9338
33	$T_{db\text{-}Adj} = 0.9315 \times T_{db\text{-}R} + 0.6602$	0.9788	$RH_{Adj} = 1.0682 \times RH_R - 15.226$	0.9787
34	$T_{db\text{-}Adj} = 0.9079 \times T_{db\text{-}R} + 0.7816$	0.9859	$RH_{Adj} = 1.1824 \times RH_R - 25.563$	0.9847
35	$T_{db\text{-}Adj} = 0.8682 \times T_{db\text{-}R} + 1.4586$	0.9843	$RH_{Adj} = 0.9528 \times RH_R - 5.2431$	0.9849
36	$T_{db\text{-}Adj} = 0.9908 \times T_{db\text{-}R} - 0.1879$	0.9783	$RH_{Adj} = 1.0916 \times RH_R - 14.711$	0.9743
37	$T_{db\text{-}Adj} = 0.9566 \times T_{db\text{-}R} + 0.4404$	0.9810	$RH_{Adj} = 1.1064 \times RH_R - 16.967$	0.9704
38	$T_{db\text{-}Adj} = 0.9191 \times T_{db\text{-}R} + 0.5877$	0.9816	$RH_{Adj} = 1.0945 \times RH_R - 11.555$	0.9791
39	$T_{db\text{-}Adj} = 0.9101 \times T_{db\text{-}R} + 0.7754$	0.9873	$RH_{Adj} = 0.9947 \times RH_R - 10.818$	0.9360
40	$T_{db\text{-}Adj} = 0.8731 \times T_{db\text{-}R} + 1.3869$	0.9850	$RH_{Adj} = 1.0296 \times RH_R - 5.3328$	0.9802
41	$T_{db\text{-}Adj} = 0.9732 \times T_{db\text{-}R} + 0.6118$	0.9846	$RH_{Adj} = 1.0001 \times RH_R - 8.5347$	0.9686
42	$T_{db\text{-}Adj} = 0.9745 \times T_{db\text{-}R} + 0.2066$	0.9794	$RH_{Adj} = 1.1552 \times RH_R - 30.174$	0.9240
43	$T_{db\text{-}Adj} = 0.9127 \times T_{db\text{-}R} + 1.1926$	0.9814	$RH_{Adj} = 1.0722 \times RH_R - 15.271$	0.9725
44	$T_{db\text{-}Adj} = 0.9114 \times T_{db\text{-}R} + 1.0636$	0.9836	$RH_{Adj} = 0.9942 \times RH_R - 9.3188$	0.9749
45	$T_{db\text{-}Adj} = 0.8748 \times T_{db\text{-}R} + 1.4462$	0.9825	$RH_{Adj} = 0.9548 \times RH_R - 2.6107$	0.9757
46	$T_{db\text{-}Adj} = 0.9563 \times T_{db\text{-}R} + 0.5488$	0.9852	$RH_{Adj} = 0.9804 \times RH_R - 7.9585$	0.9694
47	$T_{db\text{-}Adj} = 0.9860 \times T_{db\text{-}R} + 0.0824$	0.9821	$RH_{Adj} = 1.0390 \times RH_R - 11.573$	0.9709
48	$T_{db\text{-}Adj} = 0.9282 \times T_{db\text{-}R} + 0.6633$	0.9803	$RH_{Adj} = 1.1384 \times RH_R - 13.574$	0.9506
49	$T_{db\text{-}Adj} = 0.9242 \times T_{db\text{-}R} + 0.7245$	0.9891	$RH_{Adj} = 1.0996 \times RH_R - 18.539$	0.9747
50	$T_{db\text{-}Adj} = 0.8838 \times T_{db\text{-}R} + 1.4488$	0.9862	$RH_{Adj} = 0.9708 \times RH_R - 4.2192$	0.9754
51	$T_{db\text{-}Adj} = 0.9853 \times T_{db\text{-}R} + 0.6378$	0.9847	$RH_{Adj} = 1.0589 \times RH_R - 10.780$	0.9613
52	$T_{db\text{-}Adj} = 0.9945 \times T_{db\text{-}R} + 0.2702$	0.9852	$RH_{Adj} = 1.0832 \times RH_R - 13.591$	0.9607
53	$T_{db\text{-}Adj} = 0.9789 \times T_{db\text{-}R} + 0.4313$	0.9835	$RH_{Adj} = 1.0536 \times RH_R - 10.890$	0.9663
54	$T_{db\text{-}Adj} = 0.9601 \times T_{db\text{-}R} + 0.4122$	0.9827	$RH_{Adj} = 1.0126 \times RH_R - 9.3971$	0.9635
55	$T_{db\text{-}Adj} = 0.9340 \times T_{db\text{-}R} + 0.4523$	0.9855	$RH_{Adj} = 1.0929 \times RH_R - 11.233$	0.9691
56 *	$T_{db\text{-}Adj} = 0.9839 \times T_{db\text{-}R} + 0.6596$	0.9849	$RH_{Adj} = 1.0642 \times RH_R - 10.695$	0.9621

* - Meteorological shelter; $T_{db\text{-}Adj}$ - dry-bulb air temperature adjusted value (°C); $T_{db\text{-}R}$ - dry-bulb air temperature value read by the DHT22 sensor (°C); RH_{Adj} - relative humidity adjusted value (%); RH_R - relative humidity value read by the DHT22 sensor (%).

Appendix B

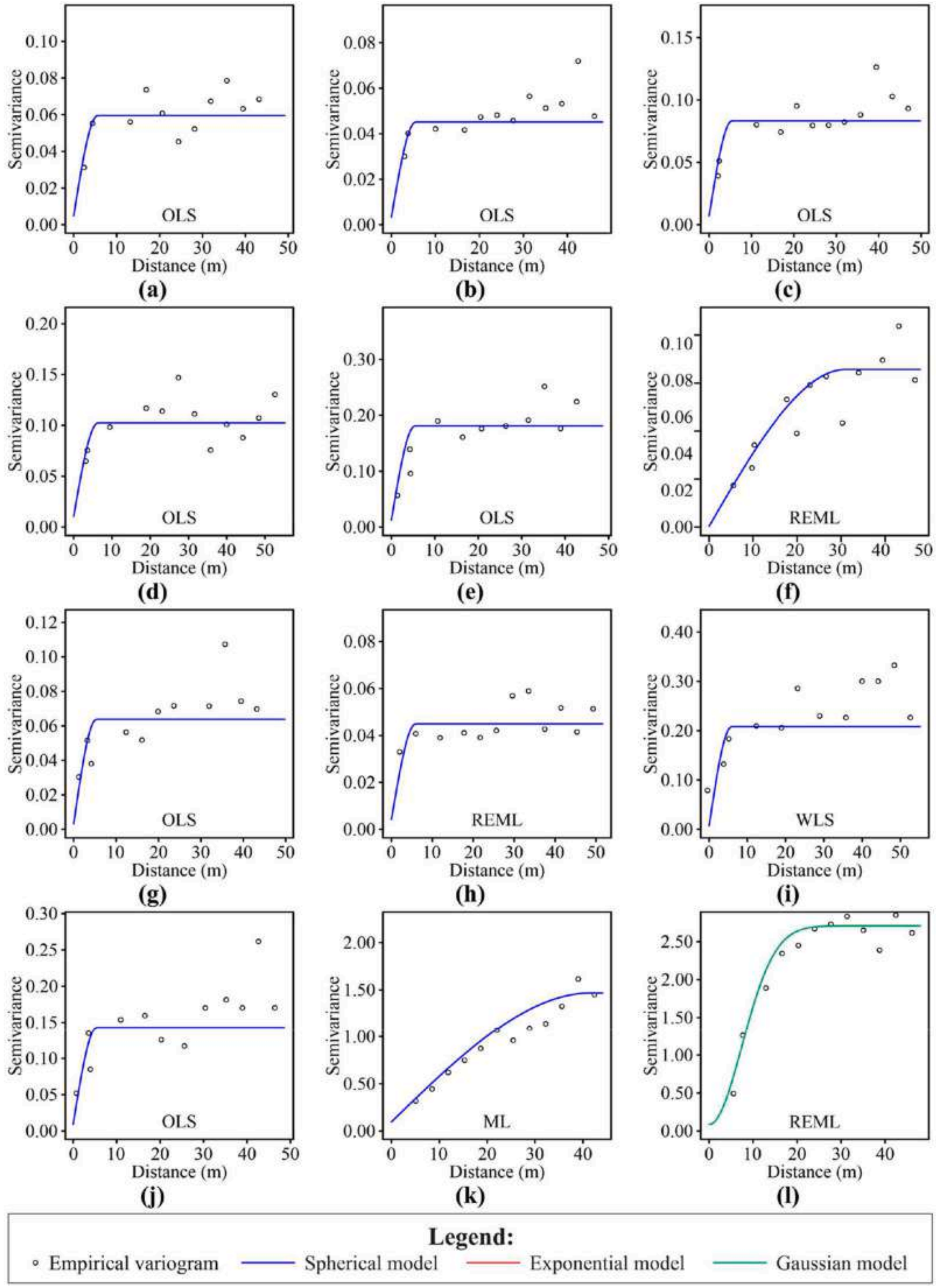

Fig. B1. Semivariograms selected based on the fitting method and model for dry-bulb air temperature (T_{db}): **(a)** dawn, **(c)** morning, **(e)** afternoon, **(g)** night, **(i)** absolute minimum and **(k)** absolute maximum in winter; and **(b)** dawn, **(d)** morning, **(f)** afternoon, **(h)** night, **(j)** absolute minimum and **(l)** absolute maximum in summer. OLS - Ordinary Least Squares; WLS - Weighted Least Squares; ML - Maximum Likelihood; and REML - Restricted Maximum Likelihood.

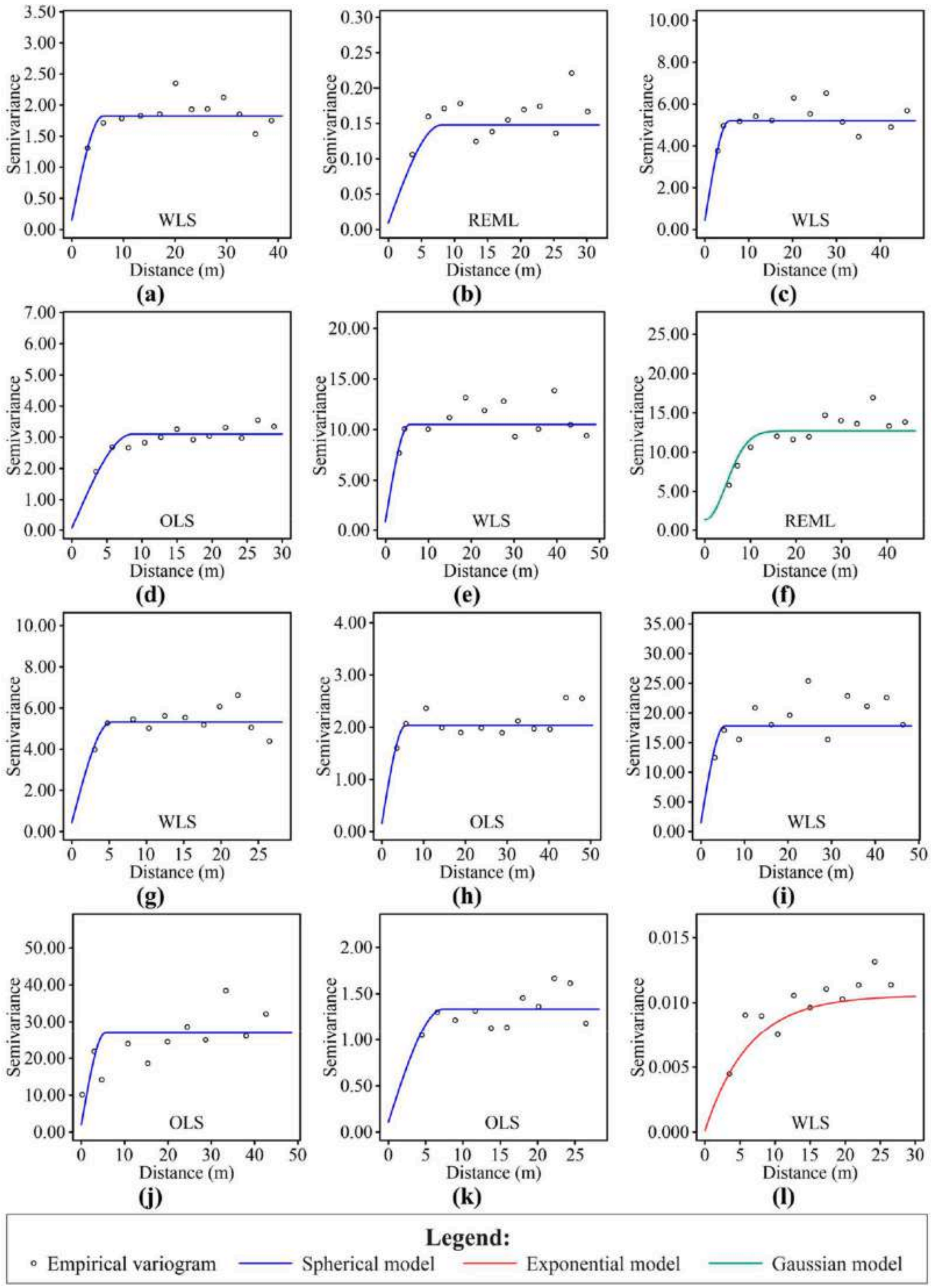

Fig. B2. Semivariograms selected based on the fitting method and model for relative humidity (RH): **(a)** dawn, **(c)** morning, **(e)** afternoon, **(g)** night, **(i)** absolute minimum and **(k)** absolute maximum in winter; and **(b)** dawn, **(d)** morning, **(f)** afternoon, **(h)** night, **(j)** absolute minimum and **(l)** absolute maximum in summer. OLS - Ordinary Least Squares; WLS - Weighted Least Squares; ML - Maximum Likelihood; and REML - Restricted Maximum Likelihood.

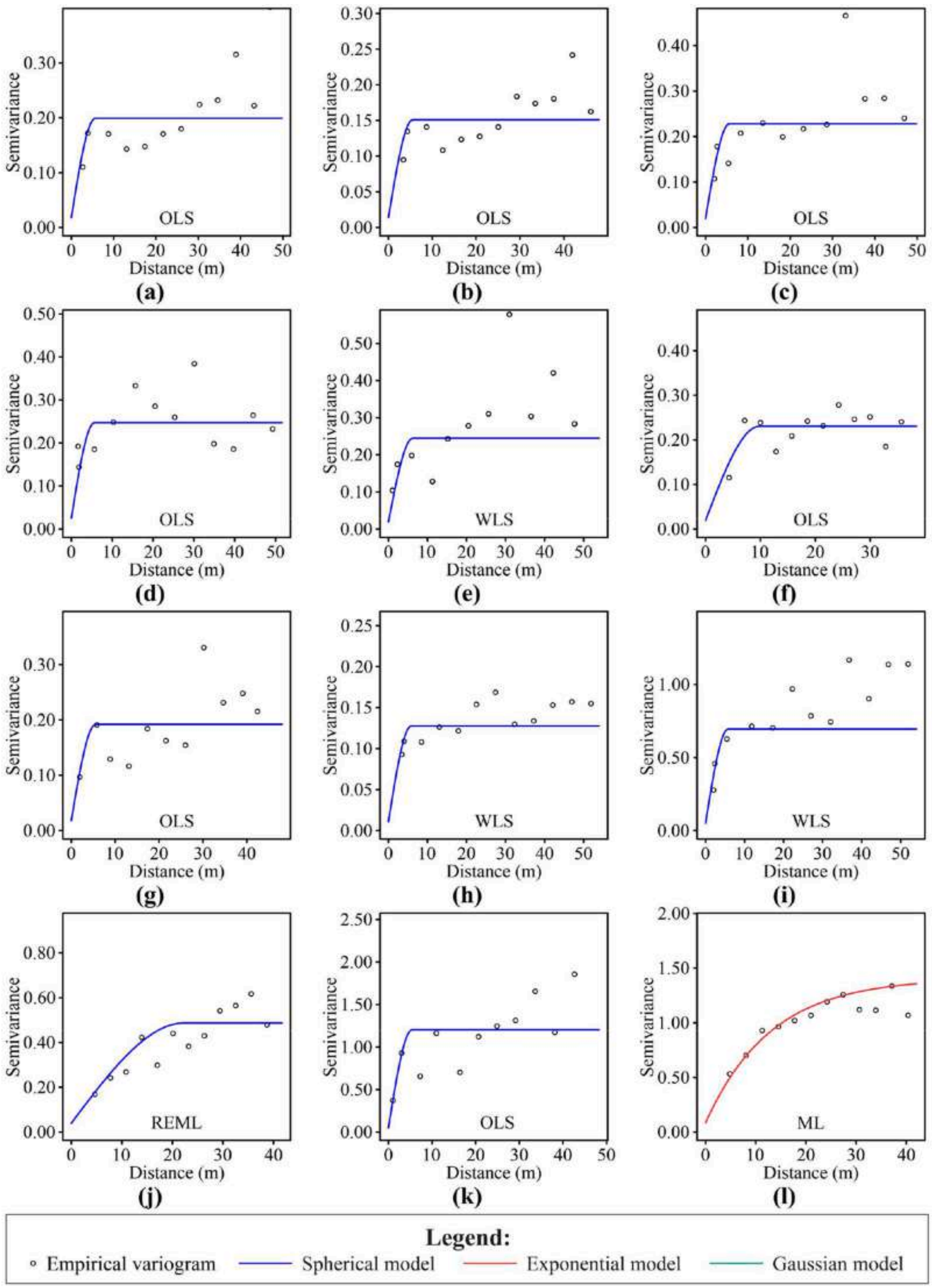

Fig. B3. Semivariograms selected based on the fitting method and model for Temperature and Humidity Index (THI): **(a)** dawn, **(c)** morning, **(e)** afternoon, **(g)** night, **(i)** absolute minimum and **(k)** absolute maximum in winter; and **(b)** dawn, **(d)** morning, **(f)** afternoon, **(h)** night, **(j)** absolute minimum and **(l)** absolute maximum in summer. OLS - Ordinary Least Squares; WLS - Weighted Least Squares; ML - Maximum Likelihood; and REML - Restricted Maximum Likelihood.

References

Allen, J. D., Hall, L. W., Collier, R. J., & Smith, J. F. (2015). Effect of core body temperature, time of day, and climate conditions on behavioral patterns of lactating dairy cows experiencing mild to moderate heat stress. *Journal of Dairy Science, 98*(1), 118–127. https://doi.org/10.3168/JDS.2013-7704

Alvares, C. A., Stape, J. L., Sentelhas, P. C., Gonçalves, J. L. M., & Sparovek, G. (2013). Köppen's climate classification map for Brazil. *Meteorologische Zeitschrift, 22*, 711–728. https://doi.org/10.1127/0941-2948/2013/0507

Andrade, R. R., Tinôco, I. F. F., Damasceno, F. A., Ferraz, G. A. S., Freitas, L. C. S. R., Ferreira, C. F. S., Barbari, M., & Teles Junior, C. G. S. (2022). Spatial analysis of microclimatic variables in compost-bedded pack barn with evaporative tunnel cooling. *Anais da Academia Brasileira de Ciências, 94*(3), Article e20210226. https://doi.org/10.1590/0001-3765202220210226

Andrade, R. R., Tinôco, I. F. F., Damasceno, F. A., Oliveira, C. E. A., Concha, M. S., Zacaroni, O. F., Bambi, G., & Barbari, M. (2024). Understanding compost-bedded pack barn systems in regions with a tropical climate: A review of the current state of the art. *Animals, 14*(12), 1755. https://doi.org/10.3390/ANI14121755

Arcidiacono, C. (2018). Engineered solutions for animal heat stress abatement in livestock buildings. *Agricultural Engineering International: CIGR Journal, Special issue: Animal Housing in Hot Climate*, 1–22. https://cigrjournal.org/index.php/Ejounral/article/view/4705.

Arshad, J., Rehman, A. U., Othman, M. T. B., Ahmad, M., Tariq, H. B., Khalid, M. A., Moosa, M. A. R., Shafiq, M., & Hamam, H. (2022). Deployment of wireless sensor network and IoT platform to implement an intelligent animal monitoring system. *Sustainability, 14*(10), 6249. https://doi.org/10.3390/SU14106249

Arulmozhi, E., Moon, B. E., Basak, J. K., Sihalath, T., Park, J., & Kim, H. T. (2021). Machine learning-based microclimate model for indoor air temperature and relative humidity prediction in a Swine Building. *Animals, 11*(1), 222. https://doi.org/10.3390/ANI11010222

Bewley, J. M., Robertson, L. M., & Eckelkamp, E. A. (2017). A 100-year review: Lactating dairy cattle housing management. *Journal of Dairy Science, 100*(12), 10418–10431. https://doi.org/10.3168/JDS.2017-13251

Biasato, I., D'Angelo, A., Bertone, I., Odore, R., & Bellino, C. (2019). Compost bedded-pack barn as an alternative housing system for dairy cattle in Italy: Effects on animal health and welfare and milk and milk product quality. *Italian Journal of Animal Science, 18*(1), 1142–1153. https://doi.org/10.1080/1828051X.2019.1623095

Blanco-Penedo, I., Ouweltjes, W., Ofner-Schröck, E., Brügemann, K., & Emanuelson, U. (2020). Symposium review: Animal welfare in free-walk systems in Europe. *Journal of Dairy Science, 103*(6), 5773–5782. https://doi.org/10.3168/JDS.2019-17315

Bleizgys, R., Naujokienė, V., & Čėsna, J. (2022). Humidification–cooling system in semi-insulated box-type cowsheds prevent the loss of milk productivity due to thermal stress. *Agronomy, 12*(5), 1131. https://doi.org/10.3390/AGRONOMY12051131

Cambardella, C. A., Moorman, T. B., Novak, J. M., Parkin, T. B., Karlen, D. L., Turco, R. F., & Konopka, A. E. (1994). Field-scale variability of soil properties in central Iowa soils. *Soil Science Society of America Journal, 58*(5), 1501–1511. https://doi.org/10.2136/SSSAJ1994.03615995005800050033X

Cartwright, S. L., Schmied, J., Livernois, A., & Mallard, B. A. (2022). Effect of In-vivo heat challenge on physiological parameters and function of peripheral blood mononuclear cells in immune phenotyped dairy cattle. *Veterinary Immunology and Immunopathology, 246*, Article 110405. https://doi.org/10.1016/J.VETIMM.2022.110405

Chang, S. C., Hsu, T. C., Chen, Y. N., & Jong, M. S. Y. (2020). The effects of spherical video-based virtual reality implementation on students' natural science learning effectiveness. *Interactive Learning Environments, 28*(7), 915–929. https://doi.org/10.1080/10494820.2018.1548490

Cheng, Q., Wang, H., Xu, X., He, T., & Chen, Z. (2024). Indoor thermal comfort sector: A review of detection and control methods for thermal environment in livestock buildings. *Sustainability, 16*(4), 1662. https://doi.org/10.3390/SU16041662

Collier, R. J., Baumgard, L. H., Zimbelman, R. B., & Xiao, Y. (2019). Heat stress: Physiology of acclimation and adaptation. *Animal Frontiers, 9*(1), 12–19. https://doi.org/10.1093/AF/VFY031

Curi, T. M. R. C., Conti, D., Vercellino, R. A., Massari, J. M., Moura, D. J., Souza, Z. M., & Montanari, R. (2017). Positioning of sensors for control of ventilation systems in broiler houses: A case study. *Scientia Agricola, 74*(2), 101–109. https://doi.org/10.1590/1678-992X-2015-0369

Dahl, G. E., & McFadden, T. B. (2022). Symposium review: Environmental effects on mammary immunity and health. *Journal of Dairy Science, 105*(10), 8586–8589. https://doi.org/10.3168/JDS.2021-21433

Damasceno, F. A. (2020). Compost barn como uma alternativa para a pecuária leiteira. In J. Amaral (Ed.), *Gulliver editora ltda* (1st ed.).

De Masi, R. F., Ruggiero, S., Tariello, F., & Vanoli, G. P. (2021). Passive envelope solutions to aid design of sustainable livestock buildings in Mediterranean climate. *Journal of Cleaner Production, 311*, Article 127444. https://doi.org/10.1016/J.JCLEPRO.2021.127444

Eckelkamp, E. A., Taraba, J. L., Akers, K. A., Harmon, R. J., & Bewley, J. M. (2016). Sand bedded freestall and compost bedded pack effects on cow hygiene, locomotion, and mastitis indicators. *Livestock Science, 190*, 48–57. https://doi.org/10.1016/J.LIVSCI.2016.06.004

Emanuelson, U., Brügemann, K., Klopčič, M., Leso, L., Ouweltjes, W., Zentner, A., & Blanco-Penedo, I. (2022). Animal health in compost-bedded pack and cubicle dairy barns in six european countries. *Animals, 12*(3), 396. https://doi.org/10.3390/ani12030396

Endres, M., Lobeck, K., Janni, K., Godden, S., & Fetrow, J. (2011). Barn environment study. In *Minnesota dairy health conference* (pp. 47–56). University of Minnesota Press.

Ferraz, G. A. S., Silva, F. M., Oliveira, M. S., Silva, F. C., & Bueno, R. L. (2014). Variabilidade espacial da força de desprendimento de frutos do cafeeiro. *Engenharia Agrícola, 34*(6), 1210–1223. https://doi.org/10.1590/S0100-69162014000600016

Ferraz, P. F. P., Ferraz, G. A. S., Damasceno, F. A., Moura, R. S., Silva, M. A. J. G., & Rodrigues, R. L. (2019). Spatial variability of enthalpy in rabbit house with and without ridge vent. *Revista Brasileira de Engenharia Agrícola e Ambiental, 23*(2), 126–132. https://doi.org/10.1590/1807-1929/AGRIAMBI.V23N2P126-132

Fick, S. E., & Hijmans, R. J. (2017). WorldClim 2: New 1-km spatial resolution climate surfaces for global land areas. *International Journal of Climatology, 37*, 4302–4315. https://doi.org/10.1002/joc.5086

Fournel, S., Ouellet, V., & Charbonneau, É. (2017). Practices for alleviating heat stress of dairy cows in humid continental climates: A literature review. *Animals, 7*(5), 37. https://doi.org/10.3390/ANI7050037

Franco, T. C. R., Ferraz, G. A. S., Carvalho, L. C. C., Silva, F. M., Alves, M. C., & Marin, D. B. (2022). Spatial variability of soil physical properties in longitudinal profiles. *Anais da Academia Brasileira de Ciências, 94*(2), Article e20200411. https://doi.org/10.1590/0001-3765202220200411

Freitas, L. C. S. R., Tinôco, I. F. F., Gates, R. S., Barbari, M., Cândido, M. G. L., & Toledo, J. V. (2019). Development and validation of a data logger for thermal characterization in laying hen facilities. *Revista Brasileira de Engenharia Agrícola e Ambiental, 23*(10), 787–793. https://doi.org/10.1590/1807-1929/agriambi.v23n10p787-793

Garcia, C. A. P., Bovo, M., Torreggiani, D., Tassinari, P., & Benni, S. (2023). 3D numerical modelling of temperature and humidity index distribution in livestock structures: A cattle-barn case study. *Journal of Agricultural Engineering, 54*(3). https://doi.org/10.4081/JAE.2023.1522

Gernand, E., König, S., & Kipp, C. (2019). Influence of on-farm measurements for heat stress indicators on dairy cow productivity, female fertility, and health. *Journal of Dairy Science, 102*(7), 6660–6671. https://doi.org/10.3168/JDS.2018-16011

Gomes, F. P. (2000). *Curso de estatística experimental* (15th ed.) FEALQ.

Guesine, G. D., Silveira, R. M. F., & Silva, I. J. O. (2023). Spatial modeling via geostatistics of the bed in a compost barn system: Thermal performance assessments. *International Journal of Biometeorology, 67*(11), 1775–1788. https://doi.org/10.1007/s00484-023-02538-9

Gunn, K. M., Holly, M. A., Veith, T. L., Buda, A. R., Prasad, R., Alan Rotz, C., Soder, K. J., & Stoner, A. M. K. (2019). Projected heat stress challenges and abatement opportunities for U.S. milk production. *PLoS One, 14*(3), Article e0214665. https://doi.org/10.1371/JOURNAL.PONE.0214665

Hahn, G. L. (1995). Environmental management for improved livestock performance, health and well-being. *Japanese Journal of Legal Medicine, 30*, 113–127. https://doi.org/10.20652/kachikukanri.30.3_113

Hahn, G. L. (1999). Dynamic responses of cattle to thermal heat loads. *Journal of Animal Science, 77*(suppl_2), 10–20. https://doi.org/10.2527/1997.77SUPPL_210X

He, J., Zhou, X., Matsui, T., Li, F., & Tanaka, T. S. T. (2022). Critical reevaluation of an efficient sampling design for assessing soil properties using bootstrap sampling and geostatistical analysis in Japanese large-scale paddy fields. *Soil Science & Plant Nutrition, 68*(5–6), 536–546. https://doi.org/10.1080/00380768.2022.2101864

Herbut, P., Angrecka, S., & Walczak, J. (2018). Environmental parameters to assessing of heat stress in dairy cattle—a review. *International Journal of Biometeorology, 62*(12), 2089–2097. https://doi.org/10.1007/s00484-018-1629-9

Herrera-González, J. L., Rodríguez-Venegas, R., Legarreta-González, M. A., Robles-Trillo, P. A., De-Santiago-Miramontes, Á., Loya-González, D., & Rodríguez-Martínez, R. (2024). Time series (ARIMA) as a tool to predict the temperature-humidity index in the dairy region of the northern desert of Mexico. *PeerJ, 12*(12), Article e18744. https://doi.org/10.7717/PEERJ.18744/SUPP-1

Isaaks, E. H., & Srivastava, R. M. (1989). *An introduction to applied geostatistics*. Oxford University Press.

Ji, B., Banhazi, T., Perano, K., Ghahramani, A., Bowtell, L., Wang, C., & Li, B. (2020). A review of measuring, assessing and mitigating heat stress in dairy cattle. *Biosystems Engineering, 199*, 4–26. https://doi.org/10.1016/J.BIOSYSTEMSENG.2020.07.009

Johann, J. A., Silva, M. C. A., Uribe-Opazo, M. A., & Dalposso, G. H. (2010). Variabilidade espacial da rentabilidade, perdas na colheita e produtividade do feijoeiro. *Engenharia Agrícola, 30*(4), 700–714. https://doi.org/10.1590/S0100-69162010000400014

Kaur, U., Malacco, V. M. R., Bai, H., Price, T. P., Datta, A., Xin, L., Sen, S., Nawrocki, R. A., Chiu, G., Sundaram, S., Min, B. C., Daniels, K. M., White, R. R., Donkin, S. S., Brito, L. F., & Voyles, R. M. (2023). Invited review: Integration of technologies and systems for precision animal agriculture—a case study on precision dairy farming. *Journal of Animal Science, 101*, 1–23. https://doi.org/10.1093/JAS/SKAD206

Kerry, R., & Oliver, M. A. (2007). Comparing sampling needs for variograms of soil properties computed by the method of moments and residual maximum likelihood. *Geoderma, 140*(4), 383–396. https://doi.org/10.1016/J.GEODERMA.2007.04.019

Kolokotroni, M., Shittu, E., Santos, T., Ramowski, L., Mollard, A., Rowe, K., Wilson, E., Filho, J. P. de B., & Novieto, D. (2018). Cool roofs: High tech low cost solution for energy efficiency and thermal comfort in low rise low income houses in high solar radiation countries. *Energy and Buildings, 176*, 58–70. https://doi.org/10.1016/J.ENBUILD.2018.07.005

Lee, J. G., Lee, S. S., Alam, M., Lee, S. M., Seong, H. S., Park, M. N., Han, S., Nguyen, H. P., Baek, M. K., Phan, A. T., Dang, C. G., & Nguyen, D. T. (2024). Utilizing 3D point cloud technology with deep learning for automated measurement and analysis of dairy cows. *Sensors, 24*(3), 987. https://doi.org/10.3390/S24030987

Leliveld, L. M. C., Brandolese, C., Grotto, M., Marinucci, A., Fossati, N., Lovarelli, D., Riva, E., & Provolo, G. (2024). Real-time automatic integrated monitoring of barn environment and dairy cattle behaviour: Technical implementation and evaluation on three commercial farms. *Computers and Electronics in Agriculture, 216*, Article 108499. https://doi.org/10.1016/J.COMPAG.2023.108499

Leso, L., Barbari, M., Lopes, M. A., Damasceno, F. A., Galama, P., Taraba, J. L., & Kuipers, A. (2020). Invited review: Compost-bedded pack barns for dairy cows. *Journal of Dairy Science, 103*(2), 1072–1099. https://doi.org/10.3168/jds.2019-16864

Li, H., Li, B., Li, H., Song, Y., & Liu, Z. (2024). Three-way k-Means model: Dynamic optimal sensor placement for efficient environment monitoring in pig house. *Animals, 14*(3), 485. https://doi.org/10.3390/ANI14030485

Llonch, L., Castillejos, L., Mainau, E., Manteca, X., & Ferret, A. (2020). Effect of forest biomass as bedding material on compost-bedded pack performance, microbial content, and behavior of nonlactating dairy cows. *Journal of Dairy Science, 0*(0). https://doi.org/10.3168/jds.2020-18496

Loukatos, D., & Arvanitis, K. G. (2021). Multi-modal sensor nodes in experimental scalable agricultural IoT application scenarios. *Lecture Notes on Data Engineering and Communications Technologies, 67*, 101–128. https://doi.org/10.1007/978-3-030-71172-6_5

Mader, T. L., Davis, M. S., & Brown-Brandl, T. (2006). Environmental factors influencing heat stress in feedlot cattle. *Journal of Animal Science, 84*(3), 712–719. https://doi.org/10.2527/2006.843712X

Matheron, G. (1962). *Traité de géostatistique appliquée* (14th ed.) (14th ed.,. *1*. Editions Technip.

McBratney, A. B., & Webster, R. (1986). Choosing functions for semi-variograms of soil properties and fitting them to sampling estimates. *Journal of Soil Science, 37*(4), 617–639. https://doi.org/10.1111/j.1365-2389.1986.tb00392.x

Messeri, A., Mancini, M., Bozzi, R., Parrini, S., Sirtori, F., Morabito, M., Crisci, A., Messeri, G., Ortolani, A., Gozzini, B., Orlandini, S., Fibbi, L., Cristofori, S., & Grifoni, D. (2023). Temperature–humidity index monitoring during two summer seasons in dairy cow sheds in Mugello (Tuscany). *International Journal of Biometeorology, 67*(10), 1555–1567. https://doi.org/10.1007/s00484-023-02510-7

Mingoti, S. A., & Rosa, G. (2008). A note on robust and non-robust variogram estimators. *Revista Escola de Minas, 61*(1), 87–95. https://doi.org/10.1590/S0370-44672008000100014

Monteiro, A. F. M., & Martins, F. B. (2019). Global solar radiation models in Minas Gerais, Southeastern Brazil. *Advances in Meteorology, 2019*(1), Article 9515430. https://doi.org/10.1155/2019/9515430

Montironi, M. A., Qian, B., & Cheng, H. H. (2017). Development and application of the ChArduino toolkit for teaching how to program Arduino boards through the C/C++ interpreter Ch. *Computer Applications in Engineering Education, 25*(6), 1053–1065. https://doi.org/10.1002/CAE.21854

Morales-Piñeyrúa, J. T., Damián, J. P., Banchero, G., & Sant'Anna, A. C. (2022). The effects of heat stress on milk production and the grazing behavior of dairy Holstein cows milked by an automatic milking system. *Journal of Animal Science, 100*(9), 1–4. https://doi.org/10.1093/JAS/SKAC225

Mota, V. C., Andrade, E. T., & Leite, D. F. (2019). Caracterização da variabilidade espacial dos índices de conforto animal em sistemas de confinamento Compost Barn. *PUBVET, 13*, 1–14. https://doi.org/10.31533/pubvet.v13n3a276.1-14

Mrema, G. C., Gumbe, L. O., Chapete, H. J., & Agullo, J. O. (2011). *Rural structures in the tropics: Design and development* (1st ed.). FAO.

Mõtus, K., Viidu, D. A., Rilanto, T., Niine, T., Orro, T., Viltrop, A., & Bougeard, S. (2024). Application of multiblock analysis to identify key areas and risk factors for dairy cow persistence. *Preventive Veterinary Medicine, 222*, Article 106081. https://doi.org/10.1016/J.PREVETMED.2023.106081

Mylostyvyi, R., Izhboldina, O., Chernenko, O., Khramkova, O., Kapshuk, N., & Hoffmann, G. (2020). Microclimate modeling in naturally ventilated dairy barns during the hot season: Checking the accuracy of forecasts. *Journal of Thermal Biology, 93*, Article 102720. https://doi.org/10.1016/J.JTHERBIO.2020.102720

Nordlund, K. V., Strassburg, P., Bennett, T. B., Oetzel, G. R., & Cook, N. B. (2019). Thermodynamics of standing and lying behavior in lactating dairy cows in freestall and parlor holding pens during conditions of heat stress. *Journal of Dairy Science, 102* (7), 6495–6507. https://doi.org/10.3168/JDS.2018-15891

Nääs, I. A. (1989). *Princípios de conforto térmico na produção animal* (1st ed.) Ícone.

Oliveira, C. E. A., Tinôco, I. F. F., Damasceno, F. A., Oliveira, V. C., Ferraz, G. A. S., Sousa, F. C., Andrade, R. R., & Barbari, M. (2022). Mapping of the thermal microenvironment for dairy cows in an open Compost-Bedded Pack Barn system with positive-pressure ventilation. *Animals, 12*(16), 2055. https://doi.org/10.3390/ANI12162055

Oliveira, C. E. A., Tinôco, I. F. F., Damasceno, F. A., Oliveira, V. C., Rodrigues, P. H. M., Ferraz, G. A. S., Sousa, F. C., Andrade, R. R., Nascimento, J. A. C., & Silva, L. F. (2023). Air velocity spatial variability in open Compost-Bedded Pack Barn system with positive pressure ventilation. *Anais da Academia Brasileira de Ciências, 95*, Article e20220415. https://doi.org/10.1590/0001-3765202320220415

Oliveira, L. R., Yanagi Junior, T., Ferraz, G. A.e. S., Yanagi, S. N. M., & Bahuti, M. (2024). Spatiotemporal variability in human thermal comfort perception in open-air spaces: Application to the state of Minas Gerais, Brazil. *International Journal of Biometeorology, 68*(3), 479–494. https://doi.org/10.1007/S00484-023-02606-0

Polsky, L., & von Keyserlingk, M. A. G. (2017). Invited review: Effects of heat stress on dairy cattle welfare. *Journal of Dairy Science, 100*(11), 8645–8657. https://doi.org/10.3168/JDS.2017-12651

Pons, M. V., Adrien, M. L., Mattiauda, D. A., Breijo, M. A., Meikle, A., Chilibroste, P., & Damián, J. P. (2023). Welfare of dairy cows in mixed feeding systems under two different conditions of confinement: Behavioral, biochemical and physiological indicators. *Applied Animal Behaviour Science, 265*, Article 105995. https://doi.org/10.1016/J.APPLANIM.2023.105995

Pramono, E. K., Karim, M. A., Fudholi, A., Bulan, R., Lapcharoensuk, R., & Sitorus, A. (2022). Low cost telemonitoring technology of semispherical solar dryer for drying arabica coffee beans. *INMATEH - Agricultural Engineering, 66*(1), 340–350. https://doi.org/10.35633/INMATEH-66-34

R Core Team. (2024). *R: A language and environment for statistical computing*. Vienna, Austria: R Foundation for Statistical Computing. Available: https://www.r-project.org/.

Renaudeau, D., Collin, A., Yahav, S., De Basilio, V., Gourdine, J. L., & Collier, R. J. (2012). Adaptation to hot climate and strategies to alleviate heat stress in livestock production. *Animal, 6*(5), 707–728. https://doi.org/10.1017/S1751731111002448

Reuscher, K. J., Cook, N. B., da Silva, T. E., Mondaca, M. R., Lutcherhand, K. M., & Van Os, J. M. C. (2023). Effect of different air speeds at cow resting height in freestalls on heat stress responses and resting behavior in lactating cows in Wisconsin. *Journal of Dairy Science, 106*(12), 9552–9567. https://doi.org/10.3168/JDS.2023-23364

Ribeiro, J. P. J., Diggle, P. J., Christensen, O., Schlather, M., Bivand, R., & Ripley, B. (2025). geoR: Analysis of geostatistical data. *R package version, 1*. https://doi.org/10.32614/CRAN.package.geoR, 9-6.

Ribeiro Júnior, P. J., & Diggle, P. J. (2001). GeoR: A package for geostatistical analysis. *R News, 1*(2), 14–18. https://ftp.uni-bayreuth.de/math/statlib/R/CRAN/doc/packages/geoR.pdf.

Rodríguez-Godina, I. J., García, J. E., Morales, J. L., Contreras, V., Véliz, F. G., Macías-Cruz, U., Avendaño-Reyes, L., & Mellado, M. (2024). Effect of heat stress during the dry period on milk yield and reproductive performance of Holstein cows. *International Journal of Biometeorology, 68*(5), 883–890. https://doi.org/10.1007/S00484-024-02633-5

Sá Júnior, A., Carvalho, L. G., Silva, F. F., & Alves, M. C. (2012). Application of the Köppen classification for climatic zoning in the state of Minas Gerais, Brazil. *Theoretical and Applied Climatology, 108*, 1–7. https://doi.org/10.1007/s00704-011-0507-8

Saitone, T. L., & Sexton, R. J. (2017). Agri-food supply chain: Evolution and performance with conflicting consumer and societal demands. *European Review of Agricultural Economics, 44*(4), 634–657. https://doi.org/10.1093/ERAE/JBX003

Sammad, A., Umer, S., Shi, R., Zhu, H., Zhao, X., & Wang, Y. (2020). Dairy cow reproduction under the influence of heat stress. *Journal of Animal Physiology and Animal Nutrition, 104*(4), 978–986. https://doi.org/10.1111/JPN.13257

Silva, M. A. J. G., Ferraz, P. F. P., Santos, L. M., Ferraz, G. A. S., Rossi, G., & Barbari, M. (2021). Effect of the spatial distribution of the temperature and humidity index in a New Zealand white rabbit house on respiratory frequency and ear surface temperature. *Animals, 11*(6), 1657. https://doi.org/10.3390/ANI11061657

Silva, M. V., Pandorfi, H., Almeida, G. L. P., Jardim, A. M. R. F., Batista, P. H. D., Silva, R. A. B., Lopes, I., Oliveira, M. E. G., Silva, J. L. B., & Moraes, A. S. (2020). Spatial variability and exploratory inference of abiotic factors in barn compost confinement for cattle in the semiarid. *Journal of Thermal Biology, 94*, Article 102782. https://doi.org/10.1016/j.jtherbio.2020.102782

Silva, M. V., Pandorfi, H., Almeida, G. L. P., Silva, R. A. B., Morales, K. R. M., Guiselini, C., Santana, T. C., Cangela, G. L. C., Barbosa Filho, J. A. D., Moraes, A. S., Montenegro, A. A. A., & Oliveira Júnior, J. F. (2023). Spatial modeling via geostatistics and infrared thermography of the skin temperature of dairy cows in a compost barn system in the Brazilian semiarid region. *Smart Agricultural Technology, 3*, Article 100078. https://doi.org/10.1016/J.ATECH.2022.100078

Smith, J. F., Bradford, B. J., Harner, J. P., Potts, J. C., Allen, J. D., Overton, M. W., Ortiz, X. A., & Collier, R. J. (2016). Short communication: Effect of cross ventilation with or without evaporative pads on core body temperature and resting time of lactating cows. *Journal of Dairy Science, 99*(2), 1495–1500. https://doi.org/10.3168/JDS.2015-9624

Tao, S., Rivas, R. M. O., Marins, T. N., Chen, Y. C., Gao, J., & Bernard, J. K. (2020). Impact of heat stress on lactational performance of dairy cows. *Theriogenology, 150*, 437–444. https://doi.org/10.1016/J.THERIOGENOLOGY.2020.02.048

Vieira, F. M. C., Soares, A. A., Herbut, P., Vismara, E. S., Godyń, D., dos Santos, A. C. Z., Lambertes, T. S., & Caetano, W. F. (2021). Spatio-thermal variability and behaviour as bio-thermal indicators of heat stress in dairy cows in a Compost Barn: A case study. *Animals, 11*(5), 1197. https://doi.org/10.3390/ani11051197

Vieira, S. R., Carvalho, J. R. P., Ceddia, M. B., & González, A. P. (2010). Detrending non stationary data for geostatistical applications. *Bragantia, 69*, 1–8. https://doi.org/10.1590/S0006-87052010000500002

Wadoux, A. M. J. C., Marchant, B. P., & Lark, R. M. (2019). Efficient sampling for geostatistical surveys. *European Journal of Soil Science, 70*(5), 975–989. https://doi.org/10.1111/EJSS.12797

Webster, R., & Oliver, M. A. (1992). Sample adequately to estimate variograms of soil properties. *Journal of Soil Science, 43*(1), 177–192. https://doi.org/10.1111/J.1365-2389.1992.TB00128.X

Webster, R., & Oliver, M. A. (2007). *Geostatistics for environmental scientists* (2nd ed.). John Wiley & Sons.

Yousef, M. K. (1985). Thermoneutral zone. In *Stress physiology in livestock. Volume I. Basic principles* (1st ed., pp. 67–73). CRC Press Inc.